



Coral reef applications of Sentinel-2: Coverage, characteristics, bathymetry and benthic mapping with comparison to Landsat 8

John D. Hedley^{a,*}, Chris Roelfsema^b, Vittorio Brando^c, Claudia Giardino^c, Tiit Kutser^d, Stuart Phinn^b, Peter J. Mumby^e, Omar Barrilero^f, Jean Laporte^g, Benjamin Koetz^h

^a Numerical Optics Ltd., Tiverton, UK

^b Remote Sensing Research Centre, School of Earth and Environmental Sciences, University of Queensland, Brisbane, Australia

^c National Research Council of Italy, Institute for Electromagnetic Sensing of the Environment, CNR-IREA, Via Bassini 15, 20133 Milano, Italy

^d Estonian Marine Institute, University of Tartu, Tallinn, Estonia

^e Marine Spatial Ecology Lab, School of Biological Sciences, University of Queensland, Brisbane, Australia

^f CS Systèmes d'Information, 5 rue Brindepont des Moulinats, 31500 Toulouse, France

^g ARGANS Ltd., Plymouth Science Park, Plymouth, UK

^h European Space Agency, Earth Observation - Department Science, Applications and Climate, Frascati, Italy



ARTICLE INFO

Keywords:

Coral reefs
Sentinel-2
Landsat
Bathymetry
Habitat mapping
Sun glint

ABSTRACT

The Sentinel-2A and 2B Multi-Spectral Instrument (MSI) offers a specification of potential value toward a number of objectives in remote sensing of coral reefs. Coral reefs represent a unique challenge for remote sensing, being highly heterogeneous at metre scales and occurring at variable depths and water clarity regimes. However, conservation initiatives, such as the United Nations Sustainable Development Goals, add urgency to the need for the large scale environmental monitoring information that remote sensing can provide. In the quest to meet this challenge a range of satellite instruments have been leveraged, from Landsat to high spatial resolution sensors such as WorldView-2, toward objectives such as: mapping of bottom types, bathymetry, change detection, and detection of coral bleaching events. Sentinel-2A and 2B offer a new paradigm of available instruments, with a 5-day revisit, 10 m multispectral spatial resolution and freely available data. Pre-launch simulation analyses by several of the authors suggested Sentinel-2 would have good performance for reef applications, in this paper we follow up on this study by reviewing the potential based on the substantial archive of actual data now available.

First we determine to what extent the World's reefs are covered by Sentinel-2, since the mission requirements do not by default include all reefs. Secondly we review how a 5-day revisit translates to a usable acquisition rate of clear images, given that cloud and surface glint are common confounding factors. The usable acquisition rate is the real determinant of the objectives to which the data can be applied. Finally we apply current processing algorithms to Sentinel-2 data of several sites over the Great Barrier Reef, including physics-based bathymetry inversion and object-orientated benthic mapping. Landsat 8 OLI is most comparable current sensor to Sentinel-2 MSI, so direct comparisons and the possibilities for data synthesis are explored.

Our findings confirm that Sentinel-2 has excellent performance for meeting several essential coral reef scientific and monitoring objectives. Taking into account cloud and sun glint, the usable acquisition rate for a large proportion of reefs is likely to be around 20 clear images a year on average, giving a new potential for evaluation of short time-scale disturbances and impacts. The spatial resolution of 10 m is a key threshold for delineating benthic features of interest such as coral structures, and there is evidence from image and field data that bleaching is detectable. Radiometrically Sentinel-2 data can support good results in physics-based methods, such as bathymetric mapping, comparable to Landsat 8 and WorldView-2. In addition the large scale acquisition area, provided by the 290 km wide swath, offers advantages over high spatial resolution imagery for mapping at multi-reef scales.

Sentinel-2 data can be immediately leveraged with existing methods, to provide a new level of reef monitoring information compared to that previously available by remote sensing. Combined with Landsat 8 and the historical Landsat archive, the data collected today will be invaluable for decades or even centuries to come. In this context, the main downside of the Sentinel-2 mission is that approximately 12% of the World's reefs currently lie outside the acquisition plan and are not imaged. Surprisingly, for a European initiative, coral reefs in

* Corresponding author.

E-mail address: j.d.hedley@numopt.com (J.D. Hedley).

European governed territories are among the worst served globally. These omissions, approximately only 1/200th of the currently imaged area, limit the global scope which otherwise would be one of Sentinel-2's greatest strengths.

1. Introduction

Coral reefs are currently under threat worldwide from numerous environmental and anthropogenic stresses (Hoegh-Guldberg et al., 2007; Pandolfi et al., 2003), and effective management and policy formation requires monitoring across all scales from local to global. While not as detailed as in-situ surveys, remote sensing provides a valuable complementary monitoring approach, in particular at large scales ($> 10^5 \text{ km}^2$) where manual surveys would be prohibitively expensive and impractical (Hedley et al., 2016). Key mapping objectives are the abundance, distribution and health of living flora and fauna, also known as the benthos, and include benthic type (e.g. coral and algae), benthic change detection and coral bleaching. These objectives require data within specific spatial and temporal ranges (Fig. 1). Geophysical parameters, such as geomorphic zonation and bathymetry, are essential inputs for the growing number of ecosystem models used in a management context (e.g. Hock et al., 2014).

Over the last forty years the number of satellite instruments available for coral reef applications has grown, starting with the early Landsat and SPOT sensors (Smith et al., 1975; Bour, 1988) and increasing rapidly in recent years with space agency platforms and commercial offerings such as the WorldView series of satellites. Sentinel-2 satellites A and B, part of the Copernicus programme headed by the European Commission in partnership with the European Space Agency (ESA), are the most recent addition, and with the Multi Spectral Imager (MSI) instrument provide a 5-day revisit, 10 m pixels in visible bands, and freely available data: specifications which cover a number of reef monitoring requirements (Fig. 1). Further, Sentinel-2 is a European mission and the physical area and biological, cultural and economic values of tropical reefs occurring in European territories are substantial. France is the fourth nation when listed by reef area, after Australia, Indonesia and the Philippines (UNEP-WCMC, 2010). The United Kingdom is 11th in the same list and has over half as many reefs as the United States. The European Union is committed to management and conservation of coral reefs through being a signatory to a number of international initiatives that specifically mention coral reefs: The United Nations Environment Assembly, The Johannesburg Declaration, Convention on Biological Diversity, and The UNESCO World Heritage Convention. In particular, a number of targets under the United Nations Sustainable Development Goal 14 (SDG 14) (oceans, seas and marine resources, <https://sustainabledevelopment.un.org/sdg14>) require region-scale information on the extent, health, resilience, and sustainability of coastal ecosystems, of which coral reefs are a key priority. The impetus for European initiatives such as Copernicus to put coral reefs central to their efforts is therefore unquestionable and the opportunity to leverage Sentinel-2 toward this aim is of great interest.

The current options for satellite based reef mapping are dominated by high spatial resolution multispectral instruments (pixels $\leq 5 \text{ m}$) and moderate resolution (pixels 10–50 m) e.g. Landsat 8 (30 m multispectral pixels). This is now changing with instruments such as Sentinel-2 and other initiatives such as the next generation of CubeSat imaging systems. While hyperspectral data is considered advantageous (Mumby et al., 1997; Hochberg and Atkinson, 2003), the drive with commercial instruments has primarily been toward very high spatial resolution multispectral data (e.g. Worldview-4, Pleiades, pixel size $\leq 2 \text{ m}$, Planet Labs constellation, 3–5 m). Coral reefs are highly heterogeneous at scales of a few meters or less (Fig. 1), differing benthic types such as corals, seagrasses or macroalgae typically occur at different spatial scales and so the optimal minimum spatial resolution may differ dependent on the objective and site (Phinn et al., 2010). High

spatial resolution offers substantial benefits, and this kind of data is widely used for one-off or occasional reef mapping exercises at local scales (Yamano, 2013). However, the expense of commercial imagery, relative infrequency of acquisition, in particular of images clear of cloud and surface glint, make it unsuitable for systematic repeated monitoring or large scale change detection. With respect to scientific missions from space agencies, coral reefs are somewhere between a land and an ocean colour application and are not specifically prioritised, so the available satellite instruments are typically a compromise toward requirements. The Landsat series has seen some use in coral reef context: freely available data facilitates the potential for global applications such as the Millennium Coral Reef Habitat Mapping Project (Andréfouët et al., 2004) and time series analysis (Palandro et al., 2008). Landsat 8 in particular, with 12-bit digitisation and the additional blue band at 443 nm which offers high depth of penetration in clear waters (Table 1), has good capability for techniques based on radiative transfer models (Giardino et al., 2016). The 16-day revisit ensures a reasonable chance of clear acquisitions several times a year, dependent on location. Capturing a 185 km wide swath means larger areas can be processed without the challenges presented when mosaicing images acquired under different conditions. While restricted by 30 m spatial resolution Landsat 8 data benefit from being the continuation of a long term dataset stretching back to the early 1980's, a requirement for analysis of long term processes (El-Askary et al., 2014). Other short term missions with hyperspectral characteristics such as Hyperion or HICO have also been tested (Kutser et al., 2006; Garcia et al., 2014a) but without a long term mission commitment these applications remain scientific investigations. Upcoming missions such as HypsIRI or EnMAP (Devred et al., 2013; Guanter et al., 2015) may reinvigorate hyperspectral reef applications but currently the options for applied benthic mapping of coral reefs by satellite instruments remain dominated high spatial resolution commercial offerings and Landsat 8.

Sentinel 2 differs significantly to the previously discussed instruments in both spatial and temporal resolution. The spatial resolution of

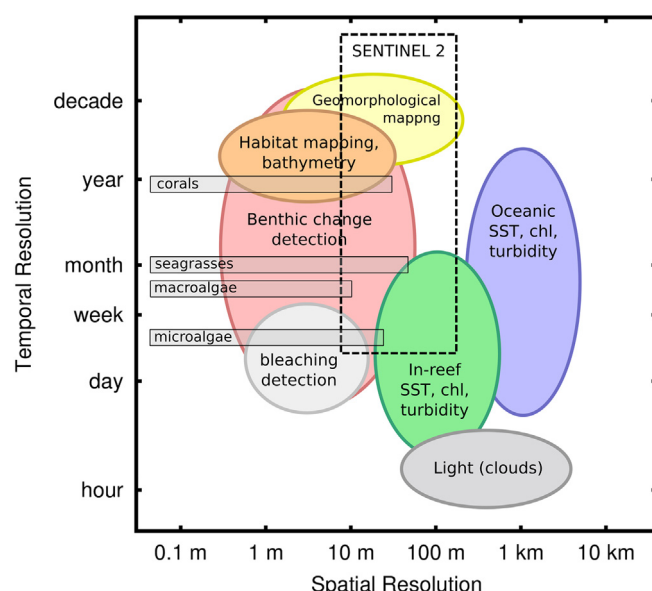


Fig. 1. The relationship between the spatial and temporal characteristics of Sentinel-2 acquisitions and the requirements for coral reef remote sensing objectives.

Table 1

Band specifications of Sentinel-2A MSI and Landsat 8 OLI. Information from: <https://earth.esa.int/web/sentinel/user-guides/sentinel-2-msi/resolutions/radiometric> and <https://landsat.gsfc.nasa.gov/landsat-8/landsat-8-bands>.

Sentinel-2A MSI			Landsat 8 OLI		
Band	Pixel size (m)	Wavelength range (nm)	Band	Pixel size (m)	Wavelength range (nm)
01	60	430–457	1	30	433–453
02	10	448–546	2	30	450–515
03	10	538–583	3	30	525–600
04	10	646–684	4	30	630–680
05	20	694–713			
06	20	731–749			
07	20	769–797			
08	10	763–908			
8A	20	848–881	5	30	845–885
09	60	932–958			
10	60	1336–1411	9	30	1360–1390
11	20	1542–1685	6	30	1560–1660
12	20	2081–2323	7	30	2100–2300
			8	15	500–680

10 m in four visible and near infra-red (NIR) bands lies directly between the ~2 m pixel high resolution sensors and the Landsat 8 multispectral bands at 30 m (Table 1). This spatial regime has not been widely used on reefs, although similar resolutions are available in the SPOT series (10 m and 6 m), and Rapid-Eye (5 m), uptake of these data for reef applications is far less than that of the commercial high resolution offerings. The 5-day revisit of the Sentinel-2A and 2B instrument pair, combined with freely available data, is unprecedented. This offers many potential benefits: from simply increased likelihood of finding imagery clear of cloud and sun glint; to high temporal resolution time series for change detection; or to new multiple-image analysis techniques. The imaging swath of Sentinel-2 at 290 km is wider than that of Landsat 8185 km, which carries the advantage of a larger simultaneous image area but with caveat of including a wider range of view angles (Roy et al., 2017). On the downside, the current Sentinel-2 mission requirements do not ensure global coverage of all reefs (nominally includes coastal areas within 20 km of landmasses > 100 km²) and this potentially undermines the advantage of free data at large scales. Additionally, unlike Landsat 8, the useful bands of Sentinel 2 are at mixed resolutions, 60 m for the equivalent of Landsat 8's deep blue band (Table 1). Pre-launch sensitivity analysis on simulated Sentinel 2 data (Hedley et al., 2012) indicated that good performance could be expected, but that mixed spatial resolutions may introduce some artefacts. In simulations spectral reflectances at 10 m resolution over dark benthic features such as corals had corresponding Band 1 values that were too high, being the average over a larger area (60 m), subsequently in a bathymetry analyses these pixels were erroneously estimated as deep water (Hedley et al., 2012). The similarity of Sentinel 2 band specification to Landsat 8 (Table 1) does however offer good possibilities for data synthesis, and may facilitate interpretation of Sentinel 2 data within the context of the Landsat historical archive if the relative performance of the sensors can be characterised.

This paper is a follow-up of the pre-launch sensitivity analysis of Hedley et al. (2012). After 18 months of operation of Sentinel-2A the imagery archive is now sufficient to review and assess the current capability and future potential for coral reef applications. The first question addressed is to what extent are the World's reefs covered by Sentinel 2 acquisitions, and where are the significant omissions, if any. Secondly, while the 5-day revisit is an impressive specification, the question of relevance to time series and change detection is how many usable images this translates to, given the possibility of cloud and water surface glint (sun glint). These factors are assessed from a series of images on the Great Barrier Reef (GBR) and with reference to a global

MODIS cloud climatology data set (Mercury et al., 2012). Finally, two frequently-used and current mapping techniques, physics-based bathymetry estimation and object-orientated bottom classification, are applied to Sentinel 2 images of sites on the GBR. The bathymetric mapping is compared directly to Landsat 8 in a parallel analysis. For the object-orientated benthic mapping both the process and results are compared to previous mapping efforts using Landsat 8 and other sensors. Some of the methods applied here are the same or similar to algorithms that will be provided in ESA's SNAP toolbox as an output of the Sen2Coral project (<http://step.esa.int/main/toolboxes/snap/>). In summary we present four analyses:

- 1) The global status of coverage of coral reefs by Sentinel-2 acquisitions.
- 2) How a 5-day revisit translates into 'usable acquisition frequency'.
- 3) Performance of physics-based bathymetry method for Sentinel-2 vs. Landsat 8.
- 4) Practicalities and results of object-orientated benthic classification using Sentinel-2 data.

The paper concludes with a summary of the benefits, and caveats, of the application of Sentinel-2 MSI data toward coral reef management objectives.

2. Methods

2.1. Global coverage estimation

The original Sentinel-2 mission requirements guaranteed only land masses > 100 km² in area, islands in the European Union and areas < 20 km from the coast (SUHET 2013). However in practice the acquisition area is larger and has been modified several times, for example the whole of the GBR is now routinely imaged. ESA does not provide an official on-going acquisition plan, therefore to assess coral reef coverage it was assumed that the combined weekly Sentinel-2A acquisition plans published by ESA in the 12 months prior to September 2017 were representative. The acquisition area was reconciled against the UNEP-WCMC Global Distribution of Coral Reefs dataset (United Nations Environment Programme - World Conservation Monitoring Centre, UNEP-WCMC, 2010). This dataset was compiled from a number of sources by UNEP-WCMC and includes data from the Millennium Coral Reef Mapping Project and the World Atlas of Coral Reefs (Spalding et al., 2001). The area of individual reefs lying inside or outside the acquisition area was quantified for each of the 85 sovereigns listed in the UNEP-WCMC dataset. To quantify the status of global coverage an analysis based on the Sentinel-2 tiling grid was conducted (SUHET, 2015), in which a list of all 110 km × 110 km Sentinel-2 tiles that contained reefs was made, and the number of those tiles that were wholly or partially missed from the acquisitions were noted. A summary of coverage is provided in the results and discussion, a report on the full analysis is supplied as supplementary information.

2.2. Usable acquisition frequency (sun glint and cloud)

Both cloud cover and surface glint are serious confounding factors for coral reef applications of remotely sensed imagery. Understanding the practical value of a 5-day revisit time requires estimating the likelihood that each image will be clear of cloud and sun-glint. The 'usable acquisition frequency' is what is relevant for time series or change detection algorithms.

With respect to cloud, first a local scale analysis was conducted using images of Heron Reef (23.442° S, 151.915° E) on the GBR. A total of 69 Sentinel-2A and Landsat 8 images acquired over a 12 month period were visually assessed as being 'clear', 'minor cloud' or 'unusable', where 'unusable' approximately corresponded to > 20% cloud cover over reef areas. Results were compared to a global seasonal cloud

cover climatology derived from 10 years of MODIS data (Mercury et al., 2012). Secondly, the Mercury et al. (2012) dataset was applied in global context by determining the percentage of global reef area under different regimes of cloud free acquisitions, using the UNEP-WCMC global reef map. I.e. to show how much of the World's reefs are cloud free 50% of the time, etc.

While correction algorithms for glint exist (Kay et al., 2009) images with minimal glint are preferred since strong correction is imperfect and introduces noise. Glint correction of Sentinel-2 data is potentially more challenging than with higher spatial resolution imagery because 10 m pixels may contain a combination of glint at different scales: 1) a component that varies pixel-to-pixel due to wave slopes spaced > 10 m apart; 2) a more constant sub-pixel component arising from surface waves smaller than 10 m. Regression based corrections (Hedley et al., 2005) fail to capture sub-pixel glint whereas statistical correction methods (Kay et al., 2009) cannot handle pixel-to-pixel variation. The frequent acquisitions of Sentinel-2 imply the best solution is simply to select images with minimal glint, so the question of interest is how frequently and under what conditions such images occur.

Surface glint is dependent on solar zenith angle, view zenith angle, relative azimuth and sea surface state (Kay et al., 2009). The brightest glint occurs when the view and solar zenith angles, and relative azimuth, are such that the view is close to the forward direct reflectance direction. Increased surface roughness widens the glint 'spot' and increase the chance of glint outside the direct reflectance direction. Sentinel-2 incident view angles vary with position in the swath with a maximum of around 12° at the edges (Roy et al., 2017). Some locations, such as part of Heron Reef, are located at swath edges in the orbit overlap area and so are imaged on two overpasses and benefit from double acquisitions. However these locations have the largest view zenith angles. Typically in one overpass the solar-view geometry will be in a forward reflectance direction (prone to glint) and in the other a reverse direction (less prone to glint). Glint is also substantially dependent on solar zenith angle which varies with season.

To estimate the frequency and conditions of glint occurrence on typical GBR sites cloud screened Sentinel-2A images of Heron Reef and Lizard Island (14.660° S, 145.459° E) were selected from an 18 month period from January 2016 to August 2017. Unlike Heron Reef, Lizard

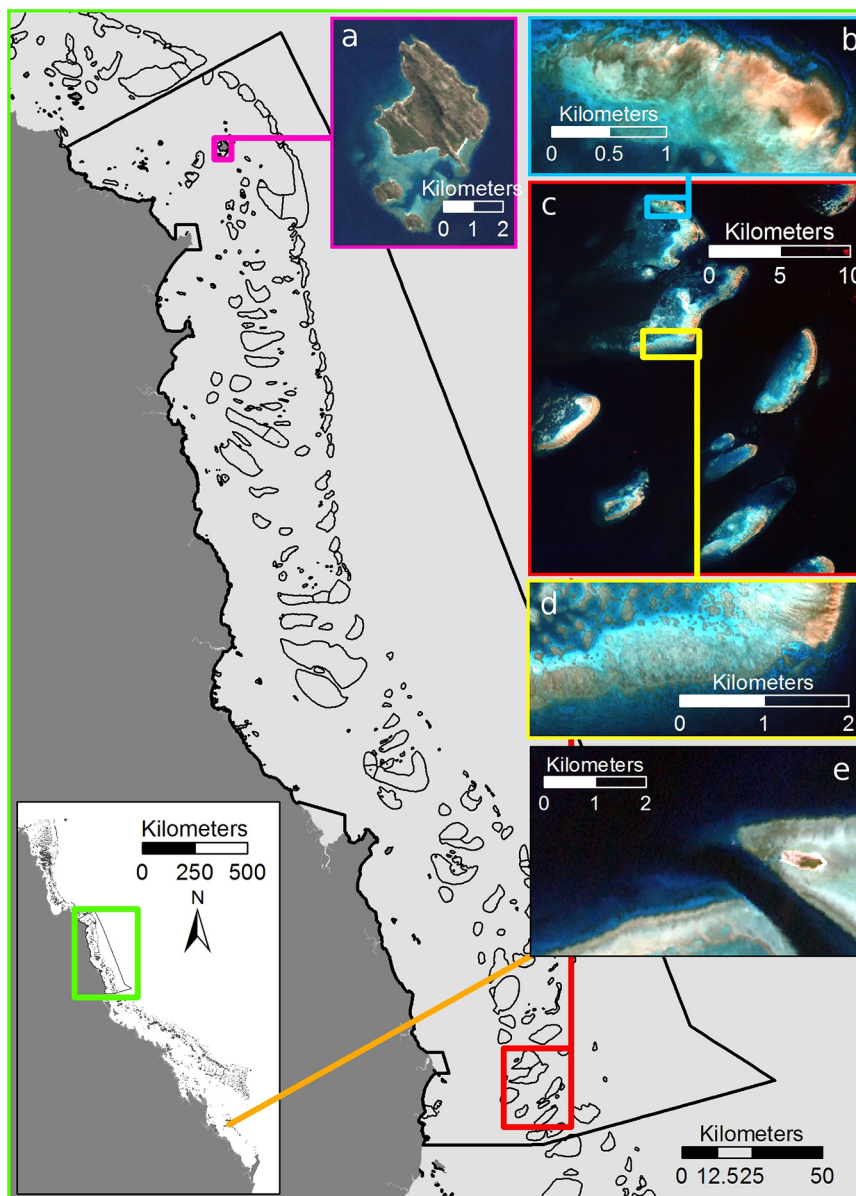


Fig. 2. Various sites on the Great Barrier Reef as referred to in this paper: (a) Lizard Island, (b) northern part of Hall-Thompson Reef, (c) SSCMR (Southern Section Cairns GBR Management Region), (d) Adelaide Reef and (e) Heron and Wistari Reefs. Images are RGB composites of bands 4, 3, and 2 of Sentinel-2A images.

Island is located closer to the centre of a swath with typical view zenith angles of $\sim 3^\circ$. Glint was estimated as the top-of-atmosphere reflectance at 660 nm (band 4 in Sentinel-2, Table 1) over deep water areas (interpretation of the atmospheric contribution is discussed in the Results section). This resulted in a total of 31 data points of solar-view geometry and top of atmosphere reflectance. These data are discussed later to provide insight on how surface glint may limit the practical usable revisit time.

2.3. Bathymetry and benthic mapping: study sites and imagery

For assessing the capability for bathymetry and benthic mapping with Sentinel-2 and Landsat 8 images were analysed from two sites on the Great Barrier Reef (GBR), Australia. The first site was used for bathymetry only: Lizard Island (14.660° S, 145.459° E) was chosen since it has a long record of scientific study and characterisation, including a substantial bathymetry dataset (Hamylton et al., 2015). The Lizard Island site is fairly small, the reef lies within an area of $7\text{ km} \times 7\text{ km}$, the Sentinel 2 image subsets analysed here being 1044×1062 pixels in the 10 m bands. The entire archive of Sentinel-2A and Landsat 8 to the start of 2015 was reviewed to find the best available images in terms of cloud cover, surface glint and atmospheric clarity. Two Sentinel-2A images and two Landsat 8 images were selected with dates of 2 July 2016, 30 August 2016, 24 July 2015 and 11 August 2016 respectively (Fig. 2a). The main aim of the analysis at this site was to compare bathymetry results between Sentinel-2A and Landsat 8 using the same methods, and to assess repeatability by using two images from each instrument.

For the second site the primary focus was benthic mapping. This site was larger, approximately $25\text{ km} \times 28\text{ km}$, and included nine reefs from further south on the GBR, in the area bounded by Ellison Reef, Gilbey Reef and Farquharson Reef (centred around 17.692° S 146.485° E, Fig. 2b). This site was chosen as it coincided with recent field data of bathymetry and benthic composition collected in the context of the Great Barrier Reef Habitat Mapping Project (Roelfsema et al., 2017, 2018, <https://www.rsrc.org.au/gbrccommon>). Henceforth this site is referred to as 'SSCMR' (Southern Section Cairns GBR Management Region). The main purpose of the analysis at the SSCMR site was to perform object orientated benthic mapping using Sentinel-2 data, to gain insight to both the required process and results in relation to the same methods using other sensors on GBR (Roelfsema et al., 2013, 2018). It was expected that the results would also be relevant for simpler mapping methods such as per-pixel classifications based on digital numbers (Andréfouët et al., 2003), which remain popular. Bathymetric analysis is an intermediate step in the object-orientated benthic mapping and this was performed for both Sentinel-2 and Landsat 8 data at the SSCMR site.

For all analyses the first five bands were used from both sensors, covering wavelengths from 433 nm to 713 nm for Sentinel 2 and 430 nm to 880 nm with Landsat 8 (Table 1). In some cases additional bands were used for glint correction (see below). For Sentinel 2 the bands at 60 m (B1) and 20 m (B5) resolution were resampled to 10 m without interpolation. The panchromatic band at 15 m resolution from Landsat 8 (band 8, Table 1) was not used due to its spectral width.

Image geo-locations were used as supplied in the level 1 data. Examination of image time series indicated level 1C Sentinel-2 images were typically geo-located within 2 pixels of each other (20 m) which is within the stated quality requirements for absolute geo-location (ESA, 2017). Improvement of geo-location through the production of the Global Reference Image (GRI) is an ongoing ESA activity (Clerc, 2017) and so was not an assessment objective within the scope of this paper. The potential consequences of geo-location error are considered in the interpretation of the results.

2.4. Bathymetry and benthic mapping: validation data

The bathymetry dataset for Lizard Island is described in detail in Hamylton et al. (2015) and consists of approximately 30,000 echo sound data points collected in December 2011 and tide corrected to a datum of mean sea level (MSL). The bathymetry data for SSCMR site was collected in 2014 using a Garmin GPS echo sounder 550C and similarly corrected to MSL, it consisted of approximately 11,000 data points.

Benthic cover data at the SSCMR site was derived from georeferenced benthic field photographs collected on dive and snorkel transects in the study area in January and May 2017. A detailed methods description is provided in (Phinn et al., 2012; Roelfsema and Phinn, 2010). Photos with 1 m^2 footprint were taken of benthos at 2–3 m intervals along transects while a GPS at the surface was tracking the position of the diver or snorkeler. Photos were assigned coordinates by synchronisation of the GPS and camera through time. Diving transects were approximately 500 m in length, conducted at depths $> 5\text{ m}$ on the reef slope and were directed to represent the main aspects of the reefs. Snorkel transects were 500–1000 m in length at 1–3 m depth and transects were directed to cross the different geomorphic zones on the reef top. Benthic composition for each individual photo was derived through automated photo analysis using CORALnet, with 3% of photos manually processed for calibration and validation of the machine learning algorithm (Beijbom et al., 2015; González-Rivero et al., 2016).

2.5. Atmospheric and glint correction

The physics-based inversion method for bathymetry described below required bottom of atmosphere spectral reflectance $R_{rs}(\lambda)$ as input, so a simple atmospheric correction (Hamylton et al., 2015) was applied to the Landsat 8 and Sentinel 2 scenes. The correction is based on look-up tables for atmospheric reflectance and transmission generated by libRadtran (Emde et al., 2016) with a maritime 99% relative humidity aerosol model as described by Antoine and Morel (1999). The look-up tables are parameterised on solar-view geometry with the only two free parameters being aerosol optical thickness: $\tau(550)$, 0 to 0.83; and wind speed: u_{10} , 0 to 10 ms^{-1} . The wind speed translates to an assumed spatially homogenous glint via the Cox-Munk equations under certain solar-view geometries (Kay et al., 2009), therefore the main effect of these two parameters is to contribute a component to the atmospheric reflectance which includes a spatially homogenous component of sea-surface reflectance. The aerosol component is typically spectrally blue and the glint component is spectrally flat. Aerosol thickness and wind speed were assumed constant over the image area and were estimated by taking one or more clear deep water areas and determining which values of $\tau(550)$ and u_{10} enabled the bathymetric model described below to correctly estimate deep water. The atmospheric correction is therefore not independent of the bathymetry analysis, the approach is closer to that of Kutser et al. (2006) where atmospheric parameters were included in the inversion, except here the atmospheric parameters were constrained to be constant over a scene.

As discussed in the last section, the spatial resolution of Sentinel 2 images and the solar-view geometry at acquisition is such that pixel-to-pixel surface glint is often visible in the 10 m bands. Although the clearest possible images were selected for this study close inspection indicated that all three Sentinel 2A scenes would benefit from per-pixel glint correction. The correction was applied according to Hedley et al. (2005), using a far red band (NIR or SWIR) to estimate and correct the glint in visible wavelength bands. Due to the differing band resolutions three steps were required: Band 1 (60 m) was corrected using Band 9, Bands 2, 3, and 4 (10 m) were corrected using Band 8, and Band 5 (20 m) was corrected using Band 7. The correction procedure was applied to Band 1 just for consistency; in practice it had very little effect because pixel-to-pixel glint was absent at the 60 m scale. The Landsat 8 scenes did not have the per-pixel glint correction applied because pixel-

to-pixel glint was not visible. Note the glint correction of the Sentinel-2A scenes was applied before the atmospheric correction described above. Note also the glint correction methodology was the same as will be made available in the ESA's SNAP toolbox an output of the Sen2Coral project.

Pahlevan et al. (2014) published a set of vicarious calibration adjustments for Landsat 8 which can be beneficial for physics-based shallow water mapping (Giardino et al., 2016). However, when tested on the imagery and methods used here, these coefficients were not of clear benefit. A similar analysis for Sentinel-2 has only just become available at the time of manuscript submission (Pahlevan et al., 2017), so the analysis presented here does not include the application of any vicarious calibration coefficients for Landsat 8 or Sentinel-2.

2.6. Bathymetry mapping

Bathymetric maps were produced using the physics based inversion method described in Hedley et al. (2009), the same approach as used in the sensitivity analysis on simulated Sentinel-2 data (Hedley et al., 2012). The method is also similar to the SWAM (Shallow Water semi-Analytical Model) implementation that will be released as part of ESA's SNAP toolbox. The basis of the method is a forward model of above water spectral remote sensing reflectance $R_{rs}(\lambda)$ based on the equations of Lee et al. (1998) of the form:

$$R_{rs}(\lambda) \approx f(P, G, X, H, e_1, e_2, m, \lambda) \quad (1)$$

where P , G , X , and H respectively represent the water column phytoplankton, coloured dissolved organic matter (CDOM), particulate backscatter and depth. The bottom reflectance is a linear mix of two endmember reflectance spectra drawn from a set of size n_e , and indexed by e_1 and e_2 such that $0 \leq e_1, e_2 < n_e$. The mix fraction of e_1 vs. e_2 is given by m which ranges from 0 to 1. Here the same six endmember spectra were used as in the previous sensitivity analysis, and included reflectances of coral, sand, algae and seagrass (Fig. 2 from Hedley et al., 2012, excluding bleached coral). At each pixel in the image a look-up-table inversion procedure (ALUT, Hedley et al., 2009) was applied to find the input values to the model which produced the closest spectral match to image reflectance. The look-up-table approach requires the parameters to lie in bounded ranges, here the limits were: phytoplankton (P) ranged from 0 to $\sim 2 \text{ mg m}^{-3}$; CDOM (G), absorption at 440 nm, $a(440)$, ranged from 0 to 0.2 m^{-1} ; Particulate backscatter at 440 nm (X) $b_{bp}(440)$ ranged from 0 to 0.1 m^{-1} ; and depth estimations were limited as being between 0 and 30 m.

To provide per-pixel bathymetry uncertainty estimates, each pixel was inverted 20 times with a random spectral error term added to the pixel reflectance derived from the covariance matrix over a deep water area (Hedley et al., 2010; Garcia et al., 2014b). This error term, the environmental noise equivalent radiance, $\text{NEAR}_{rs}(\lambda)$, (Brando et al., 2009) notionally includes all sources of pixel-to-pixel variation from the water surface upwards. The forward model had no terms to accommodate such variations so they are effectively noise. Typically this noise term is dominated by variable water surface reflectance (even after glint correction) but may also contain atmospheric fluctuations and instrument noise. The best estimate for the bathymetry at each pixel was taken as the mean over the 20 inversions and the 90% confidence intervals for bathymetry were taken as the range after discarding the highest and the lowest estimate. Tide correction for the time of image acquisition was applied using the OTPS2 tide model (Egbert and Erofeeva, 2002) assuming that a single tide estimation near the centre of the scene was representative over the entire area. All results are presented relative to mean sea level (MSL).

2.7. Sentinel-2A relative spectral response function

The atmospheric correction values and reflectance model (Eq. 1) were evaluated at 2 nm intervals and then convolved by the sensor band

relative spectral response (RSR) functions for application to imagery. This approach is in theory more accurate than convolving to band RSRs first and performing calculations in 'band space', since the bands can be wide and may encompass spectral features that combine non-linearly (e.g. Sentinel-2A Band 2 is 470–524 nm, at full width half maximum). However, in the development of this work it was deduced that there was an issue with the published Sentinel-2A RSR for Band 2. In short, initially a box function was used and gave good results, when the published RSR was implemented the results became substantially worse. Also, the published RSR for Sentinel-2A Band 2 had an unusual almost triangular shape whereas for Sentinel-2B the Band 2 RSR appeared more typical and closer to a box function. Enquiries to the Sentinel technical support team confirmed that there was a known issue with the published Sentinel-2A Band 2 RSR. This has recently been stated in the September 2017 Data Quality Report (Clerc, 2017) with the advice to use the Sentinel-2B RSR, and this is what was done. It solved the issue and is the basis of all the results presented here. The most recent update is that since the initial submission of this paper an updated Sentinel-2A RSR has been published by ESA and is indeed much more similar to the Sentinel-2B RSR in Bands 1 and 2 (March 2018 Data Quality Report, Clerc, 2018).

2.8. Benthic mapping

For the Sentinel 2 benthic mapping analysis at the SSCMR site an image dated 22 September 2015 was used, being completely cloud free for the nine reefs within the area. The image was used to produce a bathymetry map, by the method described above, and also a water column corrected bottom reflectance image, i.e. $p(\lambda)$ in the five image bands, for input to the object-orientated classifier. The estimate of bottom reflectance in each pixel was given by re-arranging the forward model equation (Eq. 3 in Hedley et al., 2009) to give $p(\lambda)$ as a function of $R_{rs}(\lambda)$ once P , G , X and H have been estimated from the inversion procedure. While the forward model contains an explicit estimate of $p(\lambda)$ from the linear mix of the endmembers (parameters e_1 , e_2 and m) this is not used directly as a bottom reflectance output because being a linear mix of a finite set of endmembers it is dimensionally constrained.

Object-based image analysis (OBIA) through Trimble eCognition 9.3 software was used to map geomorphic zones and benthic cover type by adaptation of a protocol developed previously and described in Roelfsema et al. (2013). The first part of the OBIA consisted of segmentation of the image into groups of pixels with similar characteristics, e.g. colour or texture, or a physical property such as water depth. This was followed by labelling of segments using a membership rule set that determined which class each segment was identified as (Blaschke, 2010). Some OBIA parameters required adjustment to correspond to the 10 m pixel size: this is part of the protocol as for example in Roelfsema et al. (2013, 2018) the OBIA was applied on high spatial resolution imagery varying from 2 to 4 m pixels, whereas for Roelfsema et al. (2018) pan sharpened Landsat 8 OLI imagery was used at 15 m pixel scale.

The following attributes were incorporated into OBIA: Sentinel-2 derived bathymetry, slope (calculated from bathymetry) and Sentinel-2 reflectances derived at the water surface and bottom. For each geomorphic zone category, a rule set was developed to assign a label to each segment based on a set of biophysical attributes such as water depth (e.g. MSL depth $> 3 \text{ m}$ implies reef top), colour (e.g. brightest colour implies sand), slope derived from water depth ($> 10^\circ$ implies slope region) and neighbourhood relationships, e.g. reef slope is adjacent to reef crest. Geomorphic zones were mapped down to 15 m depth using the at-surface reflectance image, water depth and slope. Dominant benthic cover type was mapped for the reef top, here defined as area above -3 m (MSL) which includes reef crest, outer and inner reef flat and shallow lagoon. Wherefore, membership rules were created based on expert knowledge of reefs, field data, bottom reflectance image and rules from previous OBIA studies (Joyce et al., 2002; Phinn

et al., 2012; Roelfsema et al., 2013, 2018). Membership rules to assign dominant benthic cover type labels to segments were based on the brightness of the segments, band ratios, segment location within each of the geomorphic zones. These rules varied between geomorphic zones dependent upon the type of relationship and/or the threshold value for a dominant benthic cover type. Dominant benthic cover type labels assigned included coral/algae, rock, rubble and sand.

3. Results and discussion

3.1. Global coral reef coverage by Sentinel-2

In total 2293 tiles are required to cover the World's reefs (Fig. 3a) of which 275 were wholly omitted in the acquisitions in the 12 month period to September 2017. A small number of reefs were missed in tiles that are partially imaged but this is a comparatively minor factor. Therefore ~12% of the tiles required for global reef coverage were missed, which is only ~1/200th of the total effort of 56,686 tiles that were imaged at least once in that period. In terms of reef area missed this also translates to 12% of the total global reef area, according to the UNEP-WCMC dataset. Here 'reef area' means the polygonal areas in the UNEP-WCMC dataset, which is primarily shallow reef areas that could be mapped by remote sensing (UNEP-WCMC et al., 2010). In many places coverage was excellent, since coral reefs are frequently associated with islands sufficiently large to be included in the Sentinel-2 land acquisition plan. Many countries had 100%, or close to, coverage of their reef areas, including the three countries with the largest reef area: Australia, Indonesia and the Philippines (with approximately 32,000 km², 20,000 km² and 12,000 km² reef area respectively). The majority of missed tiles are over small islands in the Pacific (Fig. 3a).

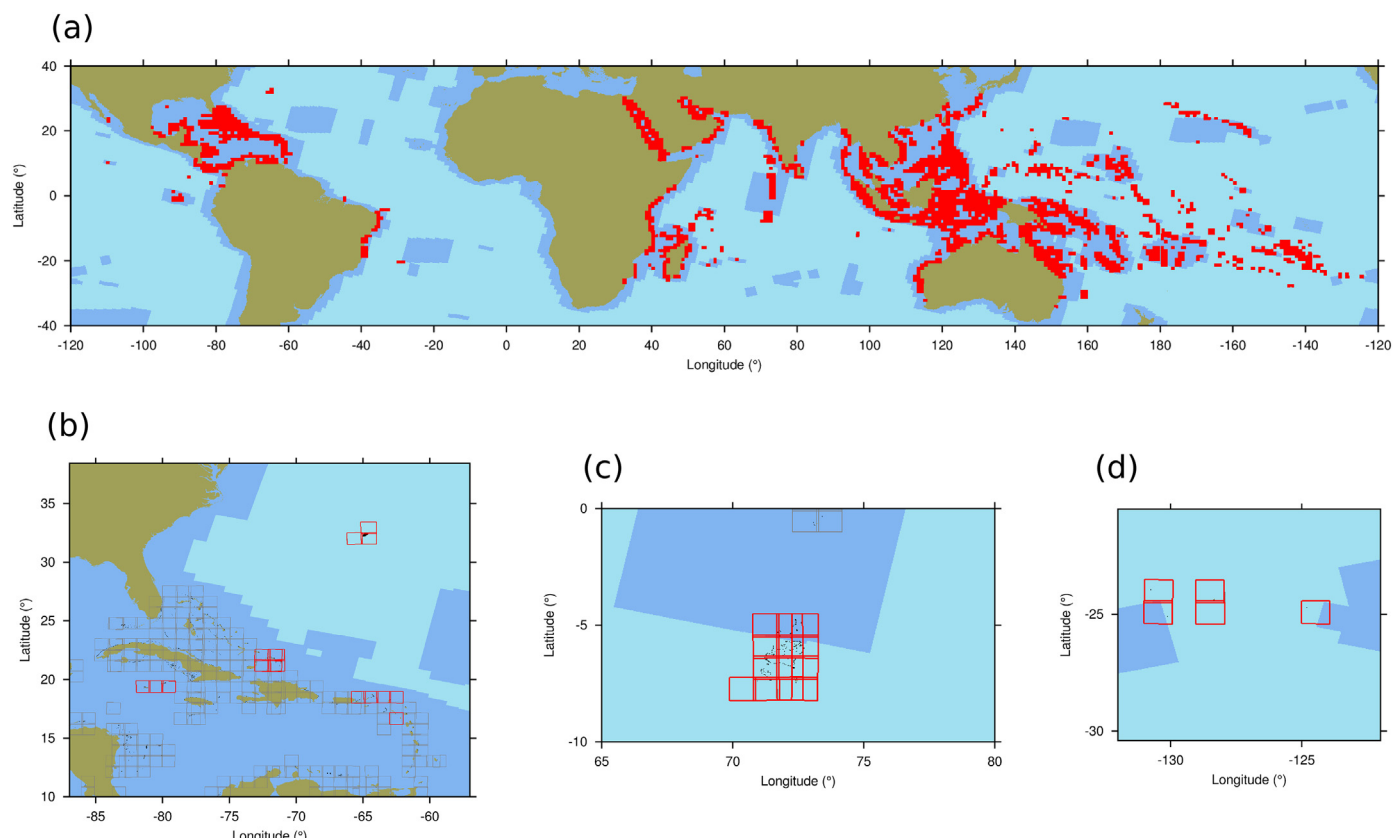


Fig. 3. (a) Global coverage of reefs by Sentinel-2A over the 12 month period to September 2017: red indicates tiles containing reefs, dark blue is acquired area. (b–d) Example detailed coverage of reefs in UK territories: black dots are reefs, red indicates tiles including reefs in UK territories, dark blue is acquired area. (b) shows omission of Bermuda, (c) Chagos Islands, (d) Pitcairn Islands. (For interpretation of the references to colour in this figure legend, the reader is referred to the web version of this article.)

Table 2

Ten least-served sovereignties ordered by physical area of reef that has not been imaged by Sentinel-2A once in the 12 months to September 2017.

Sovereignty	Total reef area	% of reef area imaged	Reef area not imaged
1 France	8296 km ²	63%	3051 km ²
2 Micronesia	3192 km ²	7%	2962 km ²
3 United States	4738 km ²	46%	2562 km ²
4 United Kingdom	2937 km ²	27%	2152 km ²
5 Kiribati	1973 km ²	5%	1873 km ²
6 Seychelles	1560 km ²	17%	1289 km ²
7 Tuvalu	879 km ²	4%	847 km ²
8 India	2036 km ²	60%	812 km ²
9 Fiji	3404 km ²	86%	483 km ²
10 New Zealand	367 km ²	14%	316 km ²

Table 2 lists the countries that have the largest coral reef areas that are not currently imaged. Interestingly, although Sentinel-2 is a European mission, and France and the United Kingdom have substantial combined reef area (~11,000 km²), European territories are among the worst served in terms of coral reef coverage (**Table 2**). Globally, around 30% of the coral reef area missed by Sentinel-2 is in European overseas territories (~5200 km²). Other poorly served territories are Micronesia, Kiribati, and Tuvalu with < 7% of their reef area imaged. The Phoenix Island group in Kiribati has the status of the largest UNESCO World Heritage site in the world, but its reefs are entirely missed. Many of the areas which are missed are those in remote and expensive to access locations, the places where satellite remote sensing offers the greatest potential (Hedley et al., 2016).

By way of specific example Fig. 3b to d illustrate the coverage of the

reefs of the United Kingdom (UK), see the supplementary information for similar plots for all 85 sovereignties listed in UNEP-WCMC dataset. While every reef area probably has special status by some criteria, it is worth noting the areas missed in Fig. 3 include Bermuda which has the northern-most coral reefs in the Atlantic (Spalding et al., 2001); the Chagos Archipelago (one of the world's largest marine reserves) and the Pitcairn Islands, a biodiversity hotspot at which 79 new species were recently discovered (Friedlander et al., 2014). While interest in the potential use of Sentinel-2 for coral reefs is likely to be high, this will be mitigated if areas of special interest are omitted from the acquisition plan.

3.2. Usable image acquisition rate (cloud and sunglint)

On average 35% of 69 acquisitions over Heron Reef in the GBR were clear of cloud but as expected there was seasonal variation, with no clear images in March to April period (Fig. 4a). Other months varied between 30% and 60% cloud free images but there is likely some statistical noise in the variation due to the small sample size ($n = 69$). The MODIS analysis of Mercury et al. (2012) matched the average cloud cover, giving 25% to 40% cloud cover with the same seasonal tendency but less pronounced (Fig. 4a). If minor cloud cover (approx. < 20% cloud over reef areas) is acceptable then on average 51% of acquisitions were usable.

Globally, the Mercury et al. (2012) dataset implies that the occurrence of cloud cover is at least 50% for almost all reefs (~95% by area), when averaged over a year (Fig. 4b). The most common annual proportion of cloud free acquisition for all reef scenes globally was 20–30%, so Heron Reef seems quite typical in this respect. Therefore due to cloud alone, a 5-day revisit more realistically will produce a 10 to 15 day on-average usable image acquisition rate with respect to Heron Reef. This figure would also seem a reasonable estimate at global scales. Although dependent on season and location, > 50% cloud-free images annually is unlikely to be achieved anywhere (effectively a 10-day revisit, Fig. 4b), but equally unlikely is < 1 in 10 images cloud free (approximately six cloud free acquisitions a year).

Solar zenith angle had a strong relation with surface glint in the Sentinel-2A data over Heron Reef and Lizard Island, assuming glint is the major contributor to top of atmosphere reflectance at 660 nm over deep water (Fig. 5). To help interpret these results, the atmospheric model used in the atmospheric correction (Section 2.5) was used to model top of atmosphere nadir reflectance over a ‘black ocean’ (includes glint but no subsurface reflectance). Reflectances were generated at 600 nm, as function of solar zenith angle and for two extreme treatments of wind speed, u_{10} , of 0 and 5 ms^{-1} paired with aerosol optical thicknesses $\tau(550)$ of 0 and 0.3 respectively (Fig. 5). The satellite data corresponded very well to the range of the modelled

reflectances, and in particular the upper bound for wind speed of 5 ms^{-1} and aerosol optical thickness of 0.3 (Fig. 5). The model and data are in agreement that minimal glint is virtually guaranteed for solar zenith angles above 40° , whereas for angles below 30° glint may or may not be present, dependent on sea state and site location in the swath. The images of Heron Reef on the west edge of the swath where relative azimuth is in the back-scatter direction were generally glint free. For those on the east edge the relative azimuth varied between 30° and 60° from direct forward reflectance and glint was in some cases very high (Fig. 5). Glint at Lizard Island, close to the swath centre and with approximately nadir view ($\sim 3^\circ$), was dependent on solar zenith angle and relative azimuth which co-varied (Fig. 5). Relative azimuth was in some cases exactly in the forward reflectance direction and this gave rise to the highest glint data points. Both images used for the bathymetry test had solar zenith angles $> 30^\circ$ and relative azimuths $> 60^\circ$ from direct reflectance direction. Note the Lizard Island outlier in Fig. 5c had substantial atmospheric haze visible over the land so this was an aerosol effect.

Overall, with respect to the sites on GBR, regardless of position in the swath, glint was minimised for solar zenith angles $> 40^\circ$, i.e. the local winter with low sun positions. This is an additional seasonal contribution to the usable image acquisition rate, but at least corresponds to a relatively cloud free period at these sites (Fig. 4a). While some glint free images were found for all positions in the swath the west edge is certainly favourable (Fig. 5). Using a glint threshold of 0.015 as ‘acceptable’ estimates the usable images due to glint as anywhere between 100% (Heron west) to 42% (five out of twelve, Lizard). Combined with the cloud free estimates from above gives a range of usable image acquisition rates from 10-day revisit (minimal cloud, no glint) giving > 30 clear images a year, to a worst case of three images a year (cloudy site, frequent glint). This worst case figure is likely overly pessimistic due to the large-scale perspective of the Mercury et al. (2012) cloud climatology, and would only apply in a very limited number of locations. Usable image rate will be seasonally variable and this may affect specific objectives, on GBR bleaching is most likely in the summer period from February to April which unfortunately coincides with periods of increased cloud and tendency for glint (Figs. 4, 5). While these estimates are very approximate they at least contextualise what a 5-day revisit may translate to locally. A ball-park figure of 20 clear images a year is certainly a reasonable a priori expectation.

3.3. Bathymetry mapping

All four bathymetric maps of Lizard Island, produced with either Sentinel-2A data or Landsat 8, were qualitatively similar at the scale of the imagery (i.e. kilometre scales). Fig. 6b illustrates one example: at this scale the visible difference in the other plots (not shown) was

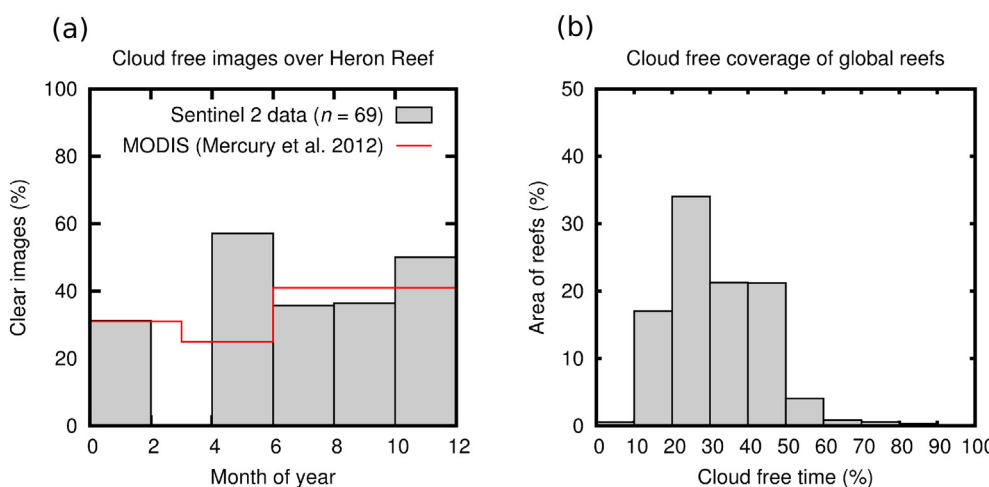


Fig. 4. (a) Frequency of cloud free Sentinel-2A images over Heron Reef in a 12 month period. Cloud free was judged subjectively as images that by visual inspection did not contain significant cloud. (b) Histogram of amount of time reefs are cloud free according to MODIS climatology analysis Mercury et al. (2012), in terms of relative reef area.

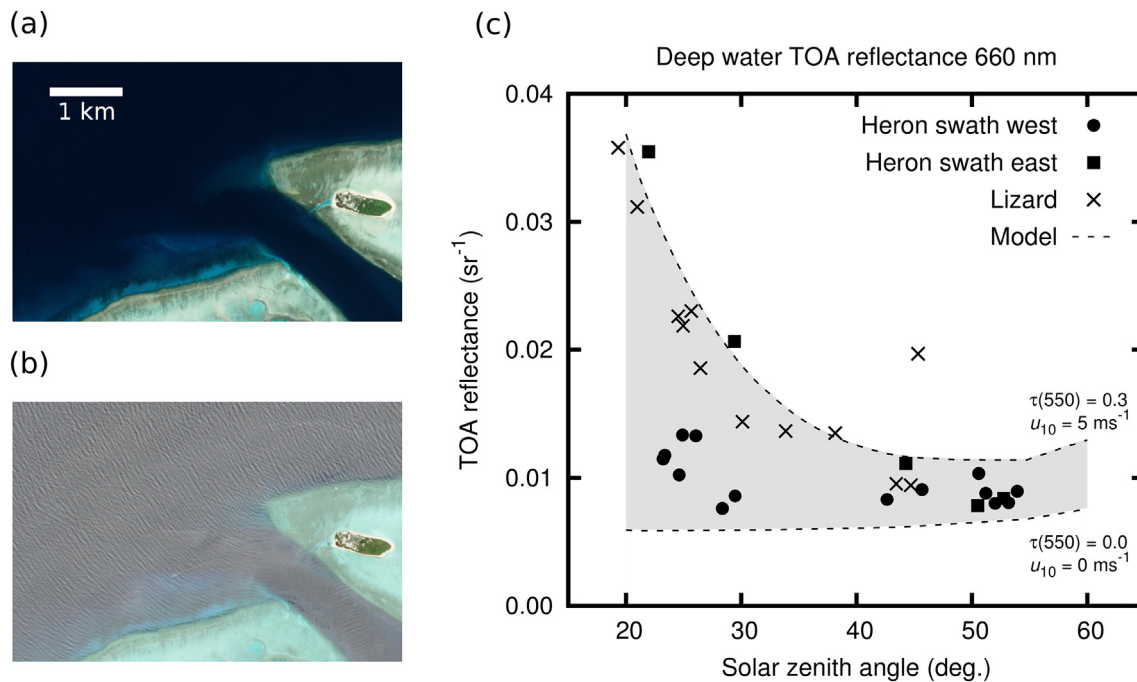


Fig. 5. Sun glint, estimated as top of atmosphere reflectance at 660 nm, as a function of solar zenith angle, assessed from (a, b) deep water areas in Sentinel-2A imagery near Heron Reef and Lizard Island, GBR. (c) Dotted lines show modelled reflectance according to the Cox-Munk equations for (lower line) a wind speed of 0 ms^{-1} (flat surface) and aerosol optical thicknesses (AOT, at 550 nm) of zero and (upper line) wind speed 5 ms^{-1} and AOT of 0.3, both with a marine 99% relative humidity aerosol model. Grey area is the possible reflectance between the model extremes. Data points come from three positions in a swath, west edge and east edge for Heron Reef and approximately central for Lizard Island. Example images are (a) low glint, swath west edge, (b) high glint, swath east edge.

primarily in the maximum depth attributed to deep water areas. In areas where the bottom is not visible the attributed depth is very sensitive to the slightest variation in image reflectances. Regression plots against the in-situ data (Fig. 7) indicate that depths were well estimated to around 15 m, and an r^2 value of 0.89 achieved with one Sentinel 2 image (Fig. 7a) is equal to that obtained in a WorldView 2 analysis with same in-situ data (Hamlyton et al., 2015). Results are possibly even better than those predicted by the simulated image analysis of Hedley et al. (2012). In that paper the equivalent analysis gave an r^2 value of 0.93 but visually the spread of points in Fig. 7a appears closer to the 1:1 line.

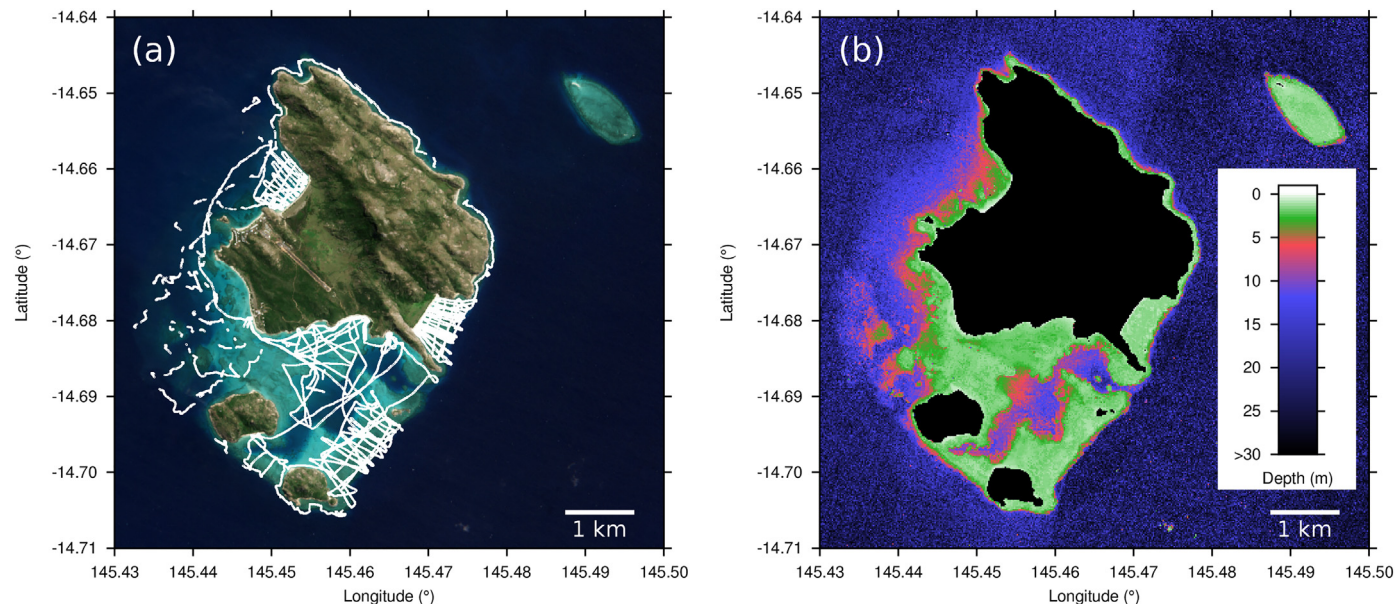


Fig. 6. (a) Location of in-situ bathymetry ground truth points at Lizard Island, (b) example bathymetric map produced from Sentinel-2A image of 21 July 2016.

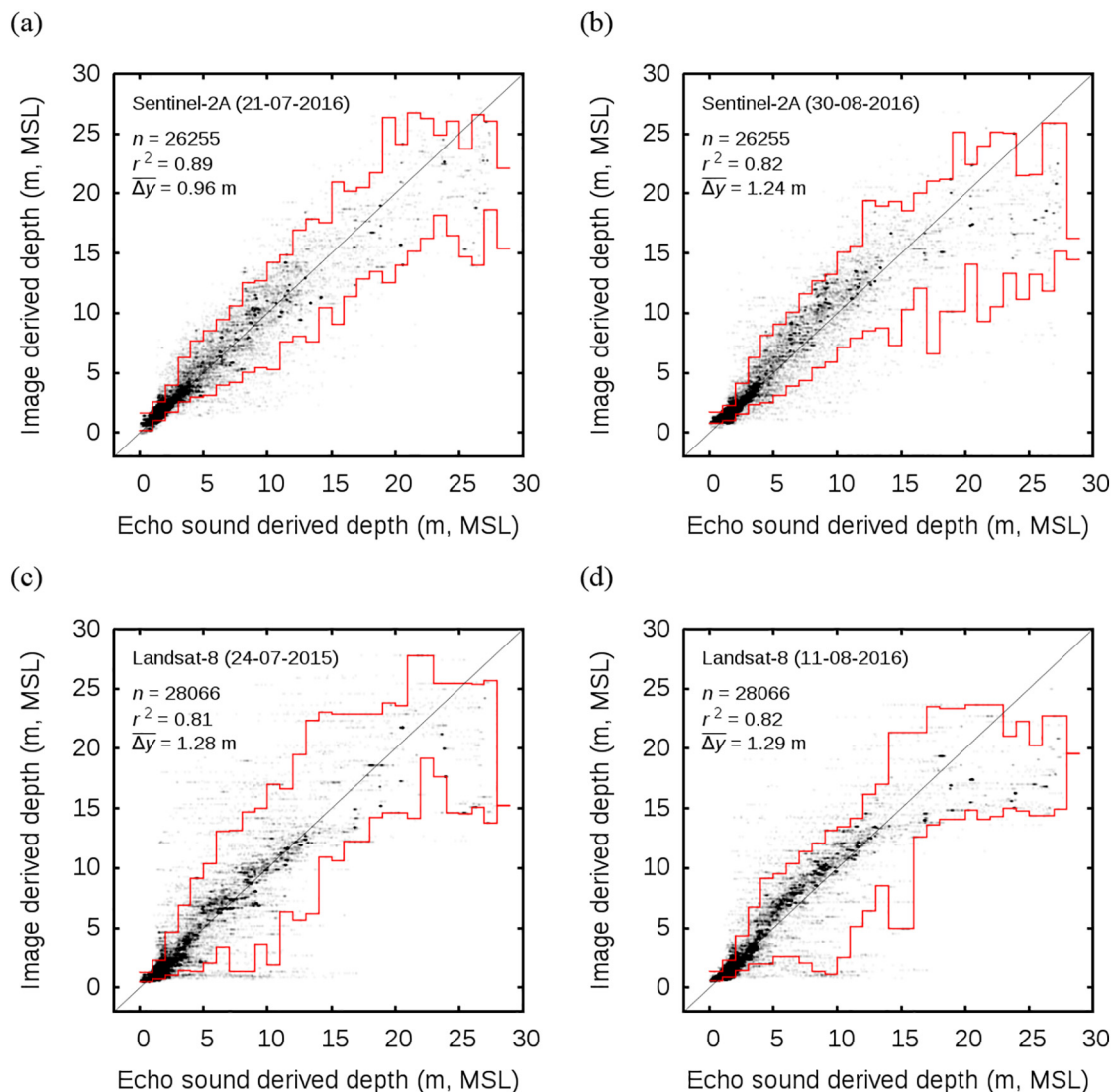


Fig. 7. Bathymetric results at Lizard Island for the two Sentinel-2A images and the two Landsat 8 images. Red lines show 90% confidence intervals from the uncertainty analysis averaged in 1 m bins. (For interpretation of the references to colour in this figure legend, the reader is referred to the web version of this article.)

the Pahlevan Landsat 8 aquatic calibration coefficients, which give a maximum adjustment of just 3.4% in Band 1 (Pahlevan et al., 2014), did not improve the result but rather introduced a systematic underestimation. With respect to the Sentinel-2 results, without using the corrected Band 2 spectral response function as described in the Methods (Section 2.7) a larger systematic error was introduced. Therefore it is clear that good correspondence to the 1:1 line in all the plots of Fig. 7 was highly dependent on the details of the calibration and atmospheric correction to within a few per cent.

The uncertainty bounds were slightly better for Sentinel-2 than Landsat 8 (Fig. 7). The propensity for very shallow image derived depths from Landsat 8 (i.e. uncertainty bounds reaching zero for depths at around 10 m) was likely due to the fact that the Sentinel-2 images were glint corrected but Landsat 8 was not. These low depth features are probably due to surface glint or white caps. While glint correction cannot effectively correct white-caps it will modify the reflectance so that those pixels are not interpreted as shallow (Hedley et al., 2005).

Image spatial resolution and geo-location of the in situ data in the imagery could also be a potential source of spread or systematic errors, particularly if the in situ data were primarily located on slopes with a certain orientation. Imagery geo-location was used as supplied in the level 1 data with no further corrections, but since the in situ data was

distributed around Lizard Island (Fig. 6a), geo-location errors probably did not introduce systematic depth errors. The higher spatial resolution of Sentinel-2 visibly affected the structure of the regression plots, since data was not grouped into 30 m pixels as it is for Landsat 8 (Fig. 7), but overall the spread of points was not appreciably less. This suggests that the bathymetric image and the in situ data cannot be reconciled at a resolution less than around 30 m. This can also be demonstrated in the bathymetry results produced for the benthic mapping exercise for the SSCMR area (Fig. 8). The initial results from Sentinel-2 exhibited quite wide spread of deviations from the 1:1 line (Fig. 8a). In this case the image geolocation was optimised by manual adjustment of up to two pixels in all directions (20 m) to maximise the r^2 value, an adjustment of one pixel proved maximal but improved the r^2 only by a tiny fraction. Applying a filter to the bathymetry image, in which each pixel became the mean of the 3×3 pixel window around it, reduced the spread in the results and substantially improved the r^2 value from 0.64 to 0.77 (Fig. 8b). This implies either that the bathymetry image contains spatial noise at the scale of 10 m, or that the in situ data is spatially noisy and not precisely geo-located at that scale, or both.

The image simulation analysis of Hedley et al. (2012) suggested that combining the 60 m resolution band with the 10 m bands for a physics-based analysis may introduce anomalies due to non-physical spectra

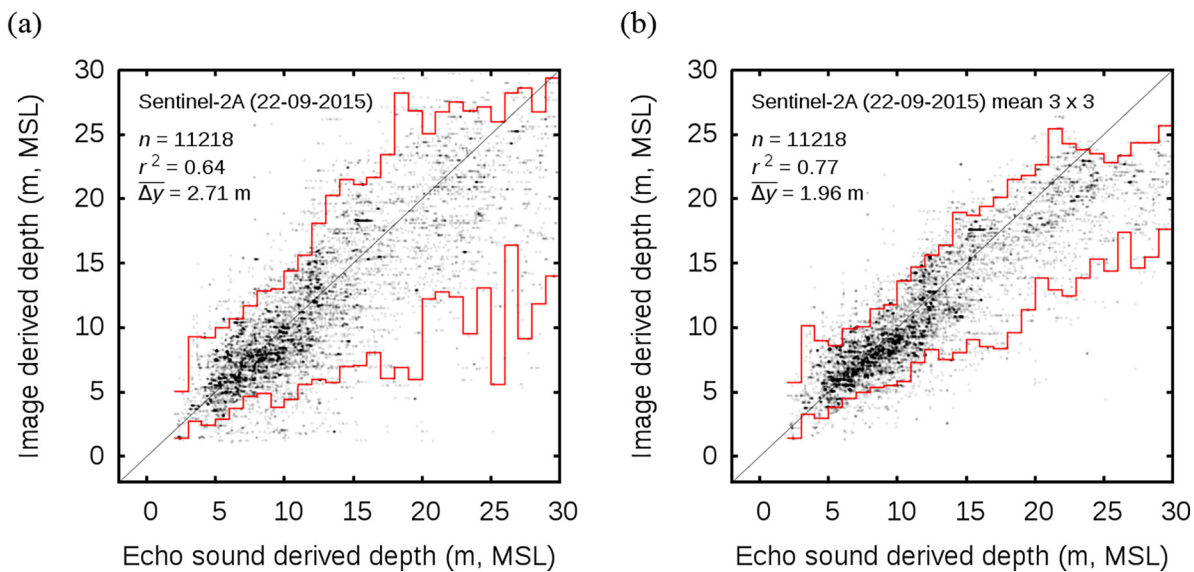


Fig. 8. Bathymetric results for SSCMR area from Sentinel-2A imagery, (a) direct results (b) results after a 3×3 pixel mean filter was applied to image output. Red lines show 90% confidence intervals from the uncertainty analysis averaged in 1 m bins. (For interpretation of the references to colour in this figure legend, the reader is referred to the web version of this article.)

over heterogeneous regions. Visual inspection of the bathymetry results (Fig. 9c) showed no evidence of serious errors due to this factor, but there were slight discontinuities present at the 60 m pixel boundaries. The previous sensitivity analysis was based on re-scaling of 1 m resolution airborne imagery and therefore pixels in the simulated image were much more sharply delineated than in real imagery, with no consideration of the instrument point spread function (PSF) (Radoux et al., 2016). Past experience with high spatial resolution imagery (pixels $\sim 2 \text{ m}$) indicates that spatial filtering frequently improves bathymetric results (unpublished data). An important general point is that the spatial resolution of a source image may not be the optimal spatial resolution for a given product produced from that image. Sentinel-2 is clearly able to resolve finer scale bathymetric features than Landsat 8 (Fig. 9c, d) but the optimal spatial resolution of the bathymetry is likely $< 10 \text{ m}$, and dependent on depth since deeper estimates are noisier (Fig. 10c). Likewise, incorporating the 15 m pixel panchromatic Landsat 8 band into the bathymetry inversion may have some influence on the effective spatial resolution, although this would be difficult to interpret since the depth estimates will be highly reliant on the differential attenuation of light in the 30 m multispectral bands.

Another issue with the SSCMR bathymetry map was that the Sentinel-2A image was acquired at the time of a relatively low tide of -0.5 m (MSL) according to OTPS2. This lead to a slight mis-correction of the shallowest areas by the deglint procedure because the water-leaving radiance in the NIR band could be non-zero. Consequentially the shallowest areas on the reef crest are estimated as slightly too deep, as can be seen in Fig. 9c vs. 9d. This was not apparent in the scatter plots (Fig. 8) since there was no in situ depth data in depths $< 5 \text{ m}$. The Lizard analyses with tides of 0.22 m and -0.19 m MSL seemed unaffected by this issue (Fig. 7). The Sentinel-2 results overall were improved by the deglint procedure so this indicates that further work on the application of this step is required.

Overall, Sentinel-2 appears equally capable of bathymetric mapping as Landsat 8, if not potentially better, both from a radiometric and spatial point of view. Within the capacity to relate in situ data to imagery it can produce results comparable to commercial sensors such as WorldView 2 (Fig. 7a vs. Hamylton et al., 2015). However physics-based inversion requires precise atmospheric corrections and calibration (Dekker et al., 2011; Goodman et al., 2008). The methods used here involved an atmospheric correction that effectively aligns the imagery to the deep water reflectance produced by the model to be

inverted; therefore objective conclusions about the calibration of the sensors or the accuracy of the atmospheric correction cannot be made. Since the only verification available for the physics-based inversion was the in situ bathymetry data intermediate results cannot be assessed. The results presented here required the best imagery, but with Sentinel-2 numerous images are available to make this choice, and that alone provides a substantial advantage. Even with the clearest images, due to the spatial resolution of Sentinel-2, per-pixel glint correction is beneficial but requires further development to reduce artefacts.

3.4. Benthic mapping

As expected, Sentinel-2 was able to resolve benthic features at smaller scales than Landsat 8. In the bottom reflectance map (Fig. 9e, f) features such as coral structures on the reef slope, which were indistinct blurs in the Landsat 8 image (upper part of Fig. 9f), were clearly delineated in the Sentinel-2 map (Fig. 9e). Equally Sentinel-2 revealed a dense population of patch reefs (bommies, $< 500 \text{ m}^2$) in places where Landsat 8 presented just a rough texture (lower left part of Fig. 9e, f). The clarity in these features was translated to the object orientated analyses of geomorphic zones and benthic type (Fig. 10). The outline of mapped features such as patch reefs or edges between sand and rock, were delineated with more detail than is typically achieved by Landsat 8 (Roelfsema et al., 2018) and represented more closely what was visible in the field or in high spatial resolution imagery such as Quickbird or Worldview 2 (Roelfsema et al., 2018). The benthic composition map for the eight reefs had overall accuracy of 49% using 6 categories which was higher than the previously conducted Landsat study with 34% (Roelfsema et al., 2018), but lower than studies on single reefs using high spatial resolution imagery. Similar improvements in accuracy can be expected for simpler per-pixel classification approaches (Andréfouët et al., 2003) since spatial delineation of benthic patches is equally important for those methods. Object based approaches can also use texture information to improve classification (Benfield et al., 2007; Saul and Purkis, 2015; Wahidin et al., 2015). So an additional advantage in the smaller pixel size of Sentinel-2 in comparison to Landsat 8 was that textures that are naturally present in reef bottom features were better visible in the Sentinel-2 imagery (Fig. 9).

Previous studies mapping geomorphic zonation using OBIA of Landsat data have used reflectance values only (Leon and Woodroffe, 2011), whereas this study included image derived attributes depth and

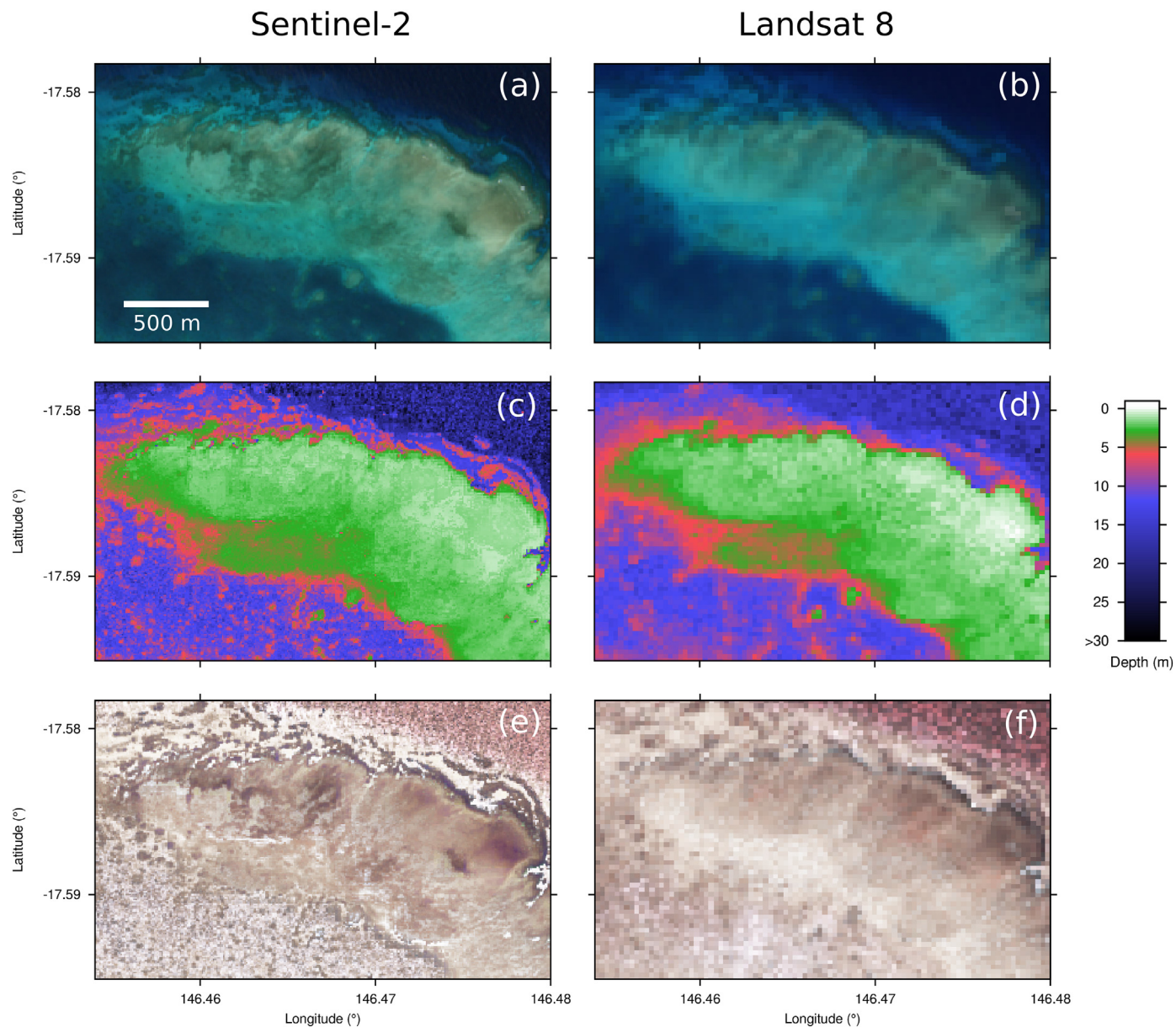


Fig. 9. Examples comparing spatial resolutions over reefs in the SSCMR region, specifically the northern part of Hall-Thompson Reef. (a, b) RGB composite from original images using bands 2, 3 and 4 of both sensors, (c, d) bathymetric map, (e, f) bottom reflectance RGB composite based on bands 1, 2 and 3.

slope, which increase the discriminatory ability and repeatability of the mapping process. The derived depth and slope attributes from Sentinel-2 are more robust than from Landsat 8 because, for example, a reef slope from 0 to 10 m depth may stretch horizontally for 50 to 100 m, which is just three Landsat 8 30 m pixels (six 15 m pan-sharpened pixels) or ten Sentinel-2 10 m multispectral pixels. Regions of slope are more reliably identifiable when characterised by more pixels, and this also applies to other geomorphological features that can be useful discriminators for benthic mapping. However, the smaller pixel size in comparison to Landsat 8 also leads to small scale pixel-to-pixel noise in the imagery, especially in deeper areas of the bathymetry and bottom reflectance layers (Fig. 9). This needs to be compensated for when applying the OBIA rule sets. The benthic mapping approaches applied in this study did not use wave exposure parameters derived from water depth as was done in the previous Landsat based study (Roelfsema et al., 2018). It is expected that this is another aspect where the gain in pixel resolution will propagate to an improved water depth and exposure model and therefore to habitat maps.

The Sentinel-2 MSI swath is 290 km wide (larger than Landsat 8's 185 km) so large areas are captured under the same environmental conditions, albeit with some variation in view angle (Roy et al., 2017). At approximately 20 km wide the eight reefs in the SSCMR site was a small subset of the available acquired area on that date. The eight reefs being within the same image allows OBIA mapping using same rule set, which is a strong advantage over high spatial resolution sensors as it improves consistency. To perform the same analysis using high spatial resolution imagery it is likely that eight individual scenes would be required, each captured under varying environmental conditions (e.g. tides, clouds, sea surface state, solar-view geometry, water clarity) and each requiring adjustment of rule sets (Phinn et al., 2012; Roelfsema et al., 2013; Saul and Purkis, 2015). Validation would also then require in situ data within each image, representing a substantially larger field work effort, whereas in this study only three out of the eight reefs were visited in the field. Therefore at larger scales (> 10 km) there are disadvantages to high spatial resolution imagery and Sentinel-2's large area acquisition may be a practical advantage.

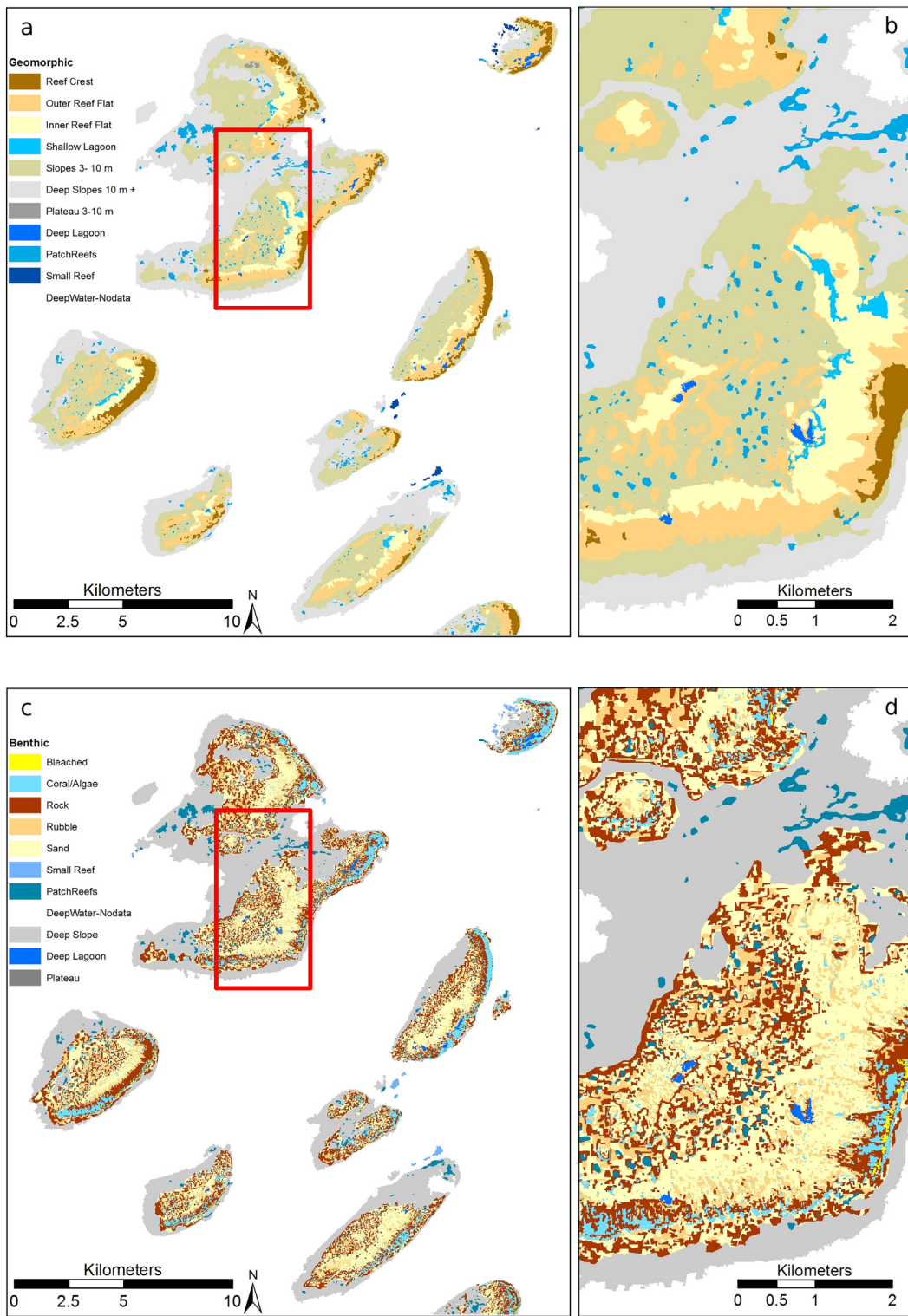


Fig. 10. (a, b) Geomorphological zone and (c, d) benthic classification maps of the SSCMR region produced by object orientated analysis of Sentinel-2 data. Panels (b, d) show zoomed in area of (a, c).

3.5. Scope for remote sensing objectives on coral reefs

The results and previous discussion highlights several distinct strengths of Sentinel-2 for reef applications, and some caveats. Table 3 summarises these findings in the context of specific objectives relevant to reef management. This section expands on the table with a brief discussion on each topic.

3.5.1. Geomorphic zone mapping

Geomorphic zones are usefully mapped at scales hundreds to thousands of meters and delineate regions at sizes of 100 s m (Figs. 1, 10). While this zonation can be captured by the spatial resolution of both Sentinel-2 and Landsat 8, Sentinel-2 can provide a finer delineation of the edges of zones. Further, geo-physical parameters such as reef slope regions can be more robustly identified with Sentinel-2 due to

Table 3

Summary of the benefits and caveats in the application of Sentinel-2 imagery towards various coral reef remote sensing objectives.

Objective	Comment
Geomorphic zone mapping	<ul style="list-style-type: none"> For large scale zones (> 100 m) Landsat 8 and Sentinel-2 equally applicable. Sentinel-2 provides better delineation and more robust identification of zones.
Benthic mapping	<ul style="list-style-type: none"> Annual or biannual maps can be created from Landsat 8 or Sentinel-2. Sentinel-2 permits mapping details that are more representative of the heterogeneous environment of reefs.
Bathymetry	<ul style="list-style-type: none"> Large area ($> 1000 \text{ km}^2$) acquisitions of Sentinel-2 are an advantage over high spatial resolution sensors for multi-reef mapping. Performance of Sentinel-2 within imagery spatial scale can be as good as Landsat 8 or high resolution sensors.
Benthic change detection	<ul style="list-style-type: none"> Repeatability, atmospheric and water surface corrections, remain an issue that requires more work, for Sentinel-2 and Landsat 8. Change detection benefits from readily available multiple images from Sentinel-2 and Landsat 8 to characterise variability baseline.
Bleaching detection	<ul style="list-style-type: none"> Cloud and surface glint limit number of usable images as a function of location and season, for both Sentinel 2 and Landsat 8. High revisit rates of Sentinel-2 and availability of imagery make bleaching detection a good prospect, Landsat-8 offers additional data. A known bleaching event appears to be visible in some Sentinel-2 imagery, further work is needed to develop methods.
Science and understanding	<ul style="list-style-type: none"> Understanding global patterns is limited by lack of global reef coverage by Sentinel-2. High revisit rates of Sentinel-2 and availability of imagery likely to foster new methods and insights.
Global scale applications	<ul style="list-style-type: none"> Long term mission commitment of Sentinel-2 and continuity with previous Landsat series data gives future potential for time series analyses over many decades. Sentinel-2 data and current methods could produce valuable new global scale information resource. Limited by lack of global reef coverage by Sentinel-2.

being covered by larger groups of pixels, and this can be beneficial for benthic mapping and other derived products such as hydrodynamic models.

3.5.2. Benthic mapping

The improved spatial resolution of Sentinel-2 over Landsat 8 is realised in features which occur at scales of around 10–100 m. These features can be better identified or more clearly mapped, such as the

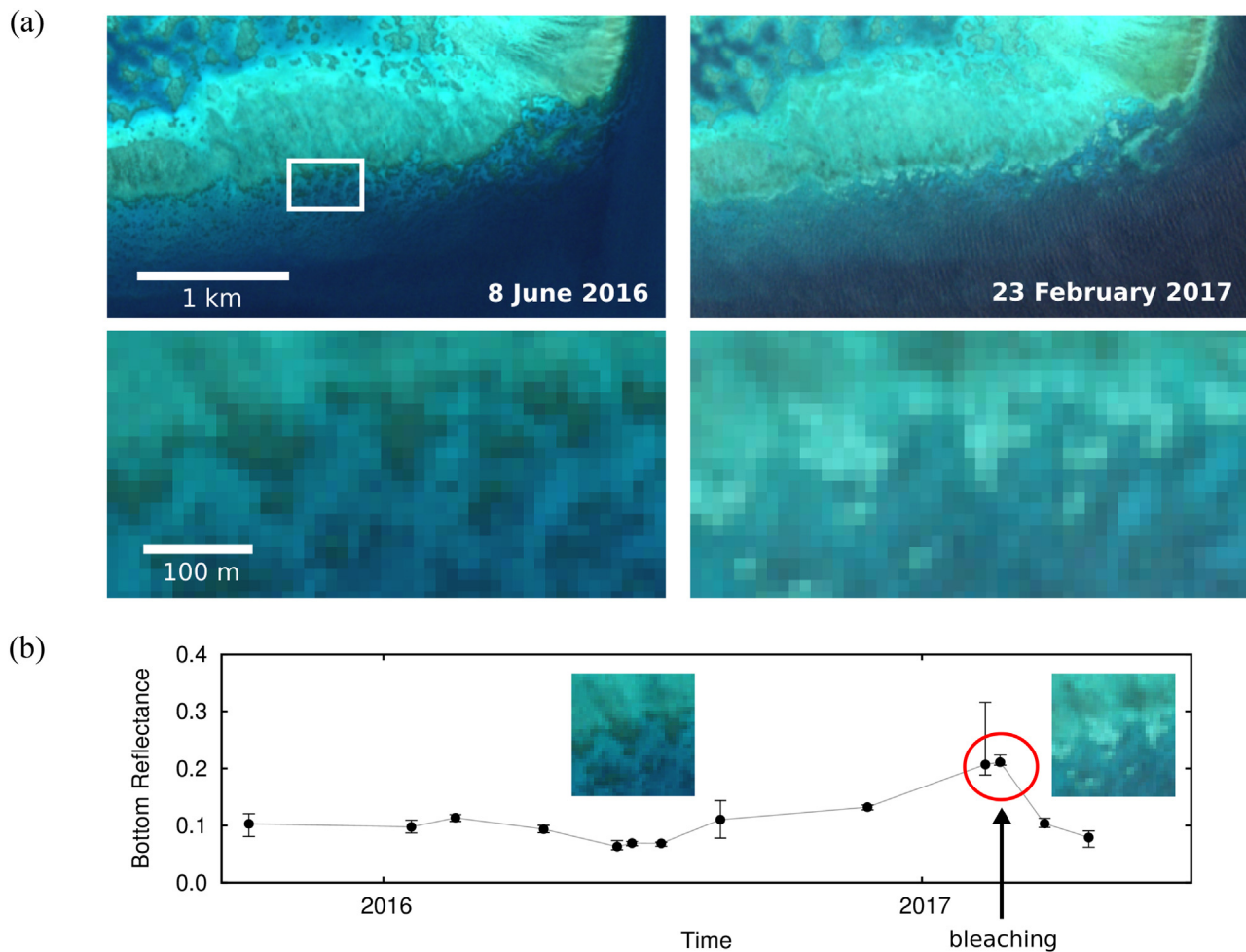


Fig. 11. (a) Bleaching as visible in Sentinel-2A imagery at Adelaide reef in February 2017, in comparison to June 2016. The two lower images show a zoomed-in area as represented by a white rectangle in top left panel. (b) Bottom reflectance at ~ 560 nm, derived as described in Section 2.8, from a time series of Sentinel-2A images over one of the bleached areas. The brightening anomaly was present in two successive images (red circle). Coral mortality at the site was verified by field surveys before and after February 2017, these data will be presented elsewhere (Roelfsema, unpublished data). (For interpretation of the references to colour in this figure legend, the reader is referred to the web version of this article.)

coral patches visible in Fig. 9e and Fig. 10. Beyond simply higher resolution maps, object orientated techniques may facilitate increasing the number of classes that can be mapped over Landsat 8 due to textures revealed at smaller scales, for example the smaller coral heads that became visible in Fig. 9e are highly characteristic. Realising the full benefit of 10 m pixel imaging requires further study on ecological spatial complexity at that scale (Lim et al., 2009). Higher spatial resolution sensors (pixels ≤ 2 m) may still be favoured for local scale mapping in areas less than $\sim 100 \text{ km}^2$ but the cost effectiveness and relative likelihood of finding clear images means Sentinel-2 will be increasingly considered as an option. Sentinel-2 is likely to find substantial use in developing countries and by NGOs with constrained budgets. One advantage over high resolution sensors is that the large acquisition area of Sentinel-2 facilitates more consistent mapping at multi-reef scales.

3.5.3. Bathymetry

Bathymetry mapping results with Sentinel-2 can be excellent in comparison with both Landsat 8 and high spatial resolution sensors. The spatial resolution of captured features is as expected, and the 60 m band is useful and appears to only induce small artefacts in otherwise noisy areas. The limiting factor in quantitative assessment of spatial features is in relating in situ data to the bathymetric maps. As with all physics-based methods, challenges remain with atmospheric and water-surface corrections. These are well known issues for all sensors (Goodman et al., 2008) but the spatial and spectral characteristics of Sentinel-2 suggest work on unique solutions are required, this work is ongoing through ESA initiatives and the scientific community (e.g. see atmospheric correction session at the EO Open Science Conference, September 2017, http://eopencience.esa.int/page_session23.php).

3.5.4. Benthic change detection

Change detection benefits greatly from multiple images to understand baseline variation, since apparent changes between any two images could be due to irrelevant causes such as tide, sea surface state, water constituents. The usable acquisition rate of Sentinel-2 is variable due to location and season, but a minimal expectation would be several good images a year. Coupled with improved spatial resolution over Landsat 8, which enables clearer identification of features, Sentinel-2 will not only be a strong choice for change detection applications but is likely to catalyse scientific developments in multi-image analysis on reefs. Currently commercial price structures and licences mean the cost of commercial high resolution imagery is prohibitive for multi-image analysis, so Sentinel-2 is a unique proposition in this application. This may change in the next five years as the traditional high spatial resolution satellite companies move to service-fee access models to match the next generation of imaging cube-sat constellations. The latter now provides accessible and useable very high spatial resolution, multi-spectral global coverage, although reef mapping applications are only just being developed (Asner et al., 2017). Change detection requires precise image alignment, and for Sentinel-2 this is ongoing work through the development of the Global Reference Image (Clerc, 2017) with a stated target image-image registration of 0.3 of a pixel (presumably only over land, ESA, 2017). Sensor performance consistency is also beneficial for change detection, and both Sentinel-2 and Landsat 8 benefit from substantial cal-val efforts from space agencies and the scientific community (Gascon et al., 2017; Pahlevan et al., 2014, 2017).

Another option to increase time series data is synthesis with Landsat 8. The methods described in this paper are equally applicable to Sentinel-2 and Landsat 8, and at the Landsat 8 spatial scale, produced similar results (Figs. 7, 9). In suitable applications Sentinel-2 and Landsat 8 data could be used side-by-side, both increasing the effective data acquisition rate but also providing a path to integrate Sentinel-2 into the legacy Landsat series data set and long term change detection analyses (Palandro et al., 2008). However, further work on this is needed since alignment of data and products even from the same image

source can be challenging.

3.5.5. Bleaching detection

Bleaching detection requires a high frequency of clear images, the onset of coral bleaching stretches over 1–4 week period, and the actual bleached white period lasts up to 4–6 weeks after which recovery or colonisation by algae returns the corals to dark reflectance. A 10 to 20-day usable image revisit should be adequate for bleaching studies and is likely achieved over many reefs, such as in the GBR area. With respect to spatial resolution and detectability, detection of bleaching by remote sensing has been demonstrated in 4 m multispectral pixel imagery (Elvidge et al., 2004; Rowlands et al., 2008), and Yamano and Tamura (2004) suggested a 25% sub-pixel bleaching area was required for detection in 30 m Landsat TM pixels. A review of Sentinel-2A imagery over GBR indicates that the 2017 bleaching event was visible at least in some locations (Fig. 11).

3.5.6. Science and understanding

At swath edges some reef locations benefit from double acquisitions, e.g. Wistari Reef to the west of Heron Island (Fig. 5). Although glint can be an issue at the eastern swath edge some images will be clear (Fig. 5c). These high frequency imaged locations will be an excellent resource for science applications, for example: understanding baseline variation for change detection algorithms; providing comparable views under different solar-view geometries (Roy et al., 2017); or simply providing substantial datasets for algorithm testing and vicarious calibration adjustments (Pahlevan et al., 2014, 2017). In general this frequency of images and spatial resolution over reefs has not been previously available, so there is an exciting opportunity to look for processes at spatial and temporal scales not previously observed.

3.5.7. Global scale applications

Reefs are under threat globally (Pandolfi et al., 2003; Wolff et al., 2015) and recent initiatives are increasing the availability of large-scale in situ data collection, including automated processing of video images for coral community composition (González-Rivero et al., 2014). The availability of such field data together with Sentinel-2 would make for an immediate and useful application: updating the global reef map of the Landsat-based Millennium Coral Reef mapping project (Andréfouët et al., 2004). That map was produced largely by visual interpretation; the application of current methods as presented in this paper could produce not just an incremental higher resolution update to the global reef map, but rather a fundamentally more comprehensive resource including geomorphic zones, benthic classification and bathymetric maps. These would form the baseline not only for cataloguing and monitoring global reefs, but a resource for ecological and biophysical models, long term change detection and understanding global scale patterns in reef ecology.

The main drawback of Sentinel-2 is the current lack of global reef coverage, this affects not only global-scale applications but many remote territories where the cost-effectiveness of remote sensing has the most to offer. Hopefully as the community develops coral reef applications of Sentinel-2 ESA and the European Commission may review the acquisition area. There may be mission constraints on what can be achieved: in some cases extending the coverage over missed reefs may simply be a case of extending the acquisition time within a swath (e.g. Chagos Islands, Fig. 3c), but for the major omissions in the Pacific additional swath segments may be required (Fig. 3d). Nevertheless, that the major omissions of an ESA mission are within European territories (Table 2) would seem a priority to address. The required additional imaging effort amounts to $\sim 1/200$ th of the current acquisitions, and would facilitate progress on European obligations to reef conservation under various environmental initiatives. Further, time is of the essence since long term data continuity is essential for change detection in the context of long term stressors such as climate change. The omitted reefs have already missed out on over 18 months of acquisitions, which in

some cases just require swaths to be extended by the equivalent of a handful of tiles (Fig. 3c).

4. Conclusions

Sentinel-2 has the capability to deliver essential scientific, monitoring and management-ready information for coral reef applications. This capability is a step up from Landsat 8 due to spatial resolution and revisit time, but Sentinel-2 also performs well in comparison high resolution imagery and offers advantages in terms of cost effectiveness and large scale coverage. Existing methods, as demonstrated here, can immediately enable effective use of Sentinel-2 by the reef science community and management agencies globally, to address their essential environmental information requirements – this also applies to hydrographic agencies, defence applications and private industry. The revisit time and cost-effectiveness of imagery is unparalleled, and offers many advantages: from simply being able to select the clearest images to opportunities for fundamentally new methods and insights. In the near future new methods are certain to be developed to meet the opportunity that Sentinel-2 presents, and this can only further add to the use of Sentinel-2 in coral reef applications. Synergy with Landsat 8, and future and past Landsat missions, also adds substantial value to Sentinel-2 data.

That nearly 90% of the World's reefs are imaged by what was envisaged as a land mission is certainly a positive outcome, but the missing 12% is likely to be a disappointment to many potential reef users. Under the current acquisition plan, many regions will not benefit from Sentinel-2 at all, and lack of global coverage is limiting for the global-scale science and management applications for which Sentinel-2 would otherwise be a very strong proposition. It is our hope that there is the possibility for ESA and the European Commission to review and extend the Sentinel-2 acquisition plan to cover more, if not all, reefs. Full coral reef coverage would remove the only obstacle for immediate uptake of Sentinel-2 in providing global-scale environmental information required to meet the European Union's conservation obligations under numerous initiatives, including the UN Sustainable Development Goals. In particular, given the surprising and substantial omission of coverage of reefs in European territories, an extended acquisition plan would be very much in line with the aims of the Copernicus programme to support Earth Observation in a European context. The true value of 100% global coverage of reefs would be fully realised in the decades and even centuries to come, when, inevitably, future conservation efforts seek to look back in time to understand long term trajectories at global scales.

Acknowledgements

The work presented here was part funded by the European Space Agency project Sen2Coral as part of the SEOM programme (S2 for Land and Water, Coral Reefs). The global coral reef map was used with kind permission of UNEP-WCMC. The bathymetry data from Lizard Island was provided by Sarah Hamylton and Rob Beaman. The Great Barrier Reef Foundation funded development work, field work and analysis related to the benthic mapping exercise. OBIA image analysis was performed with eCognition and software support was provided by Trimble. Fieldwork and field data analysis could not have been done without the help of volunteer field teams and the charter vessel MV Kalinda.

Appendix A. Supplementary data

Supplementary data to this article can be found online at <https://doi.org/10.1016/j.rse.2018.07.014>.

References

- Andréfouët, S., Kramer, P., Torres-Pulliza, D., Joyce, K.E., Hochberg, E.J., Garza-Pérez, R., et al., 2003. Multi-site evaluation of IKONOS for classification of tropical coral reef environments. *Remote Sens. Environ.* 88, 128–143.
- Andréfouët, S., Muller-Karger, F.E., Robinson, J.A., Kranenburg, C.J., Torres-Pulliza, D., Spraggins, S., Murch, B., 2004. Global assessment of modern coral reef extent and diversity for regional science and management applications: a view from space. In: Proceedings of the 10th International Coral Reef Symposium, Okinawa, Japan, 28 June–2 July 2004.
- Antoine, D., Morel, A., 1999. A multiple scattering algorithm for atmospheric correction of remotely sensed ocean colour (MERIS instrument): principle and implementation for atmospheres carrying various aerosols including absorbing ones. *Int. J. Remote Sens.* 20, 1875–1916.
- Asner, G.P., Martin, R.E., Mascaro, J., 2017. Coral reef atoll assessment in the South China Sea using planet dove satellites. *Remote Sens. Ecol. Conserv.* 3, 57–65.
- Beijbom, O., Edmunds, P.J., Roelfsema, C., Smith, J., Kline, D.I., Neal, B.P., Dunlap, M.J., Moriarty, V., Fan, T.-Y., Tan, C.-J., Chan, S., Treibitz, T., Gamst, A., Mitchell, B.G., Kriegman, D., 2015. Towards automated annotation of benthic survey images: variability of human experts and operational modes of automation. *PLoS One* 10, e0130312.
- Benfield, S.L., Guzman, H.M., Mair, J.M., Young, J.A.T., 2007. Mapping the distribution of coral reefs and associated sublitoral habitats in Pacific Panama: a comparison of optical satellite sensors and classification methodologies. *Int. J. Remote Sens.* 28, 5047–5070.
- Blaschke, T., 2010. Object based image analysis for remote sensing. *J. Photogramm. Remote Sens.* 65, 2–16.
- Bour, W., 1988. SPOT images for a coral reef mapping in New Caledonia. A fruitful approach for classic and new topics. In: Proceedings of the 6th International Coral Reef Symposium, Australia, 1988. vol. 2. pp. 445–448.
- Brando, V.E., Anstee, J.M., Wettle, M., Dekker, A.G., Phinn, S.R., Roelfsema, C., 2009. A physics based retrieval and quality assessment of bathymetry from suboptimal hyperspectral data. *Remote Sens. Environ.* 113, 755–770.
- Clerc, S., 2017. S2 MPC data quality report. In: S2-PDGS-MPC-DQR Issue 19 (06/09/2017). European Space Agency. <https://earth.esa.int/web/sentinel/user-guides/sentinel-2-msi/document-library>.
- Clerc, S., 2018. S2 MPC data quality report. In: S2-PDGS-MPC-DQR Issue 25 (06/03/2018). European Space Agency. <https://earth.esa.int/web/sentinel/user-guides/sentinel-2-msi/document-library>.
- Dekker, A.G., Phinn, S.R., Anstee, J., Bissett, P., Brando, V.E., Casey, B., Fearn, P., Hedley, J., Klonowski, W., Lee, Z.P., Lynch, M., 2011. Intercomparison of shallow water bathymetry, hydro-optics, and benthos mapping techniques in Australian and Caribbean coastal environments. *Limnol. Oceanogr. Methods* 9, 396–425.
- Devred, E., Turpie, K.R., Moses, W., Klemas, V.V., Moisan, T., Babin, M., Toro-Farmer, G., Forget, M.-H., Young-Heon, J., 2013. Future retrievals of water column bio-optical properties using the hyperspectral infrared imager (HypSIRI). *Remote Sens.* 5, 6812–6837. <https://doi.org/10.3390/rs5126812>.
- Egbert, G.D., Erofeeva, S.Y., 2002. Efficient inverse modeling of barotropic ocean tides. *J. Atmos. Ocean. Technol.* 19, 183204. [https://doi.org/10.1175/1520-0426\(2002\)019<1832:EIMOOB>2.0.CO;2](https://doi.org/10.1175/1520-0426(2002)019<1832:EIMOOB>2.0.CO;2).
- El-Askary, H., Abd El-Mawla, S.H., Li, J., El-Hattab, M.M., El-Raey, M., 2014. Change detection of coral reef habitat using Landsat-5 TM, Landsat 7 ETM+ and Landsat 8 OLI data in the Red Sea (Hurghada, Egypt). *Int. J. Remote Sens.* 35, 2327–2346.
- Elvidge, C.D., Dietz, J.B., Berkelmans, R., Andréfouët, S., Skirving, W., Strong, A.E., Tuttle, B.T., 2004. Satellite observation of Keppel Islands (Great Barrier Reef) 2002 coral bleaching using IKONOS data. *Coral Reefs* 23, 123–132.
- Emde, C., Buras-Schnell, R., Kylling, A., Mayer, B., Gasteiger, J., Hamann, U., Kylling, J., Richter, B., Pause, C., Dowling, T., Bugliaro, L., 2016. The libRadtran software package for radiative transfer calculations (version 2.0.1). *Geosci. Model Dev.* 9, 1647–1672. <https://doi.org/10.5194/gmd-9-1647-2016>.
- ESA, 2017. Sentinel-2 MSI Technical Guide. <https://earth.esa.int/web/sentinel/technical-guides/sentinel-2-msi>.
- Friedlander, A.M., Caselle, J.E., Ballesteros, E., Brown, E.K., Turchik, A., Sala, E., 2014. The real bounty: marine biodiversity in the Pitcairn Islands. *PLoS One* 9 (6), e100142. <https://doi.org/10.1371/journal.pone.0100142>.
- Garcia, R., Fearn, P., McKenna, L.I.W., 2014a. Detecting trend and seasonal changes in bathymetry derived from HICO imagery: a case study of Shark Bay, Western Australia. *Remote Sens. Environ.* 147, 186–205.
- Garcia, R.A., McKenna, L.I.W., Hedley, J.D., Fearn, P.R.C.S., 2014b. Improving the optimization solution for a semi-analytical shallow water inversion model in the presence of spectrally correlated noise. *Limnol. Oceanogr. Methods* 12, 651–669. <https://doi.org/10.1016/j.jrse.2014.03.010>.
- Gascon, F., Bouzinac, C., Thépaut, O., Jung, M., Francesconi, B., Louis, J., et al., 2017. Copernicus sentinel-2A calibration and products validation status. *Remote Sens.* 9, 584. <https://doi.org/10.3390/rs9060584>.
- Giardino, C., Bresciani, M., Fava, F., Matta, E., Brando, V.E., Colombo, R., 2016. Mapping submerged habitats and mangroves of Lampi Island Marine National Park (Myanmar) from in situ and satellite observations. *Remote Sens.* 8, 2. <https://doi.org/10.3390/rs8010002>.
- González-Rivero, M., Bongaerts, P., Beijbom, O., Pizarro, O., Friedman, A., Rodriguez-Ramírez, A., Upcroft, B., Laffoley, D., Kline, D., Vevers, R., et al., 2014. The Catlin seaview survey—kilometre-scale seascape assessment, and monitoring of coral reef ecosystems. *Aquat. Conserv. Mar. Freshwat. Ecosyst.* 24, 184–198.
- González-Rivero, M., Beijbom, O., Rodriguez-Ramírez, A., Holtrop, T., González-Marrero, Y., Ganase, A., Roelfsema, C., Phinn, S., Hoegh-Guldberg, O., 2016. Scaling up

- ecological measurements of coral reefs using semi-automated field image collection and analysis. *Remote Sens.* 8, 30.
- Goodman, J.A., Lee, Z.P., Ustin, S.L., 2008. Influence of atmospheric and sea-surface corrections on retrieval of bottom depth and reflectance using a semi-analytical model: a case study in Kaneohe Bay, Hawaii. *Appl. Opt.* 47, F1–F11.
- Guanter, L., Kauffmann, H., Segl, K., Foerster, S., Rogass, C., et al., 2015. The EnMAP spaceborne imaging spectroscopy mission for Earth observation. *Remote Sens.* 7, 8830–8857. <https://doi.org/10.3390/rs70708830>.
- Hamilton, S.M., Hedley, J.D., Beaman, R.J., 2015. Derivation of high-resolution bathymetry from multispectral satellite imagery: a comparison of empirical and optimisation methods through geographical error analysis. *Remote Sens.* 7, 16257–16273. <https://doi.org/10.3390/rs71215829>.
- Hedley, J.D., Harborne, A.R., Mumby, P.J., 2005. Simple and robust removal of sun glint for mapping shallow-water benthos. *Int. J. Remote Sens.* 26, 2107–2112.
- Hedley, J.D., Roelfsema, C., Phinn, S.R., 2009. Efficient radiative transfer model inversion for remote sensing applications. *Remote Sens. Environ.* 113, 2527–2532.
- Hedley, J.D., Roelfsema, C., Phinn, S., 2010. Propagating uncertainty through a shallow water mapping algorithm based on radiative transfer model inversion. In: Proceedings of the Ocean Optics XX Conference, Anchorage, AK, USA, 27 September–1 October 2010.
- Hedley, J.D., Roelfsema, C., Koetz, B., Phinn, S., 2012. Capability of the sentinel 2 mission for tropical coral reef mapping and coral bleaching detection. *Remote Sens. Environ.* 120, 145–155. <https://doi.org/10.1016/j.rse.2011.06.028>.
- Hedley, J.D., Roelfsema, C.M., Chollett, I., Harborne, A.R., Heron, S.F., Weeks, S., Skirving, W.J., Strong, A.E., Eakin, C.M., Christensen, T.R.L., Tizzon, V., Bejerano, S., Mumby, P.J., 2016. Remote sensing of coral reefs for monitoring and management: a review. *Remote Sens.* 8, 118–157.
- Hochberg, E.J., Atkinson, M.J., 2003. Capabilities of remote sensors to classify coral, algae, and sand as pure and mixed spectra. *Remote Sens. Environ.* 85, 174–189.
- Hock, K., Wolff, N.H., Condie, S.A., Anthony, K.R.N., Mumby, P.J., Paynter, Q., 2014. Connectivity networks reveal the risks of crown-of-thorns starfish outbreaks on the Great Barrier Reef. *J. Appl. Ecol.* 51, 1188–1196.
- Hoegh-Guldberg, O., Mumby, P.J., Hooten, A.J., Steneck, R.S., Greenfield, P., Gomez, E., et al., 2007. Coral reefs under rapid climate change and ocean acidification. *Science* 318, 1737–1742.
- Joyce, K., Phinn, S., Roelfsema, C., Neil, D., Dennison, W., 2002. Mapping the southern Great Barrier Reef using Landsat ETM and the Reef Check classification scheme. In: 11th Australasian Remote Sensing & Photogrammetry Conference. Causal Publications, pp. 239–250.
- Kay, S., Hedley, J.D., Lavender, S., 2009. Sun glint correction of high and low spatial resolution images of aquatic scenes: a review of methods for visible and near-infrared wavelengths. *Remote Sens.* 1, 697–730.
- Kutser, T., Miller, I.R., Jupp, D.L.B., 2006. Mapping coral reef benthic substrates using hyperspectral space-borne images and spectral libraries. *Estuar. Coast. Shelf Sci.* 70, 449–460.
- Lee, Z., Carder, K.L., Mobley, C.D., Steward, R.G., Patch, J.S., 1998. Hyperspectral remote sensing for shallow waters: 1. A semianalytical model. *Appl. Opt.* 37, 6329–6338.
- Leon, J., Woodroffe, C.D., 2011. Improving the synoptic mapping of coral reef geomorphology using object-based image analysis. *Int. J. Geogr. Inf. Sci.* 25, 949–969.
- Lim, A., Hedley, J.D., Ledrew, E., Mumby, P.J., Roelfsema, C., 2009. The effects of ecologically determined spatial complexity on the classification accuracy of simulated coral reef images. *Remote Sens. Environ.* 113, 965–978.
- Mercury, M., Green, R., Hook, S., Oaida, B., Wu, W., Gunderson, A., Chodas, M., 2012. Global cloud cover for assessment of optical satellite observation opportunities: a HypsIPI case study. *Remote Sens. Environ.* 126, 62–71. <https://doi.org/10.1016/j.rse.2012.08.007>.
- Mumby, P.J., Green, E.P., Edwards, A.J., Clark, C.D., 1997. Coral reef habitat-mapping: how much detail can remote sensing provide? *Mar. Biol.* 130, 193–202. <https://doi.org/10.1007/s002270050238>.
- Pahlevan, N., Lee, Z., Wei, J., Schaaf, C.B., Schott, J.R., Berk, A., 2014. On-orbit radiometric characterization of OLI (Landsat-8) for applications in aquatic remote sensing. *Remote Sens. Environ.* 154, 272–284.
- Pahlevan, N., Sarkar, S., Franz, B.A., Balasubramanian, S.V., He, J., 2017. Sentinel-2 MultiSpectral instrument (MSI) data processing for aquatic science applications: demonstrations and validations. *Remote Sens. Environ.* 201, 47–56.
- Palandro, D.A., Andréfouët, S., Hu, C., Hallock, P., Muller-Karger, F., Dustan, P., Callahan, M.K., Kranenburg, C., Beaver, C.R., 2008. Quantification of two decades of shallow-water coral reef habitat decline in the Florida Keys National Marine Sanctuary using Landsat data (1984–2002). *Remote Sens. Environ.* 112, 3388–3399. <https://doi.org/10.1016/j.rse.2008.02.015>.
- Pandolfi, J.M., Bradbury, R.H., Sala, E., Hughes, T.P., Bjorndal, K.A., Cooke, R.G., McArdele, D., McClenachan, L., Newman, M.J.H., Paredes, G., et al., 2003. Global trajectories of the long-term decline of coral reef ecosystems. *Science* 301, 955–958. <https://doi.org/10.1126/science.1085706>.
- Phinn, S.R., Roelfsema, C.M., Stumpf, R., 2010. Remote sensing: discerning the promise from the reality. In: Longstaff, B.J., Carruthers, T.J.B., Dennison, W.C., Lookingbill, T.R., Hawkey, J.M., Thomas, J.E., Wicks, E.C., Woerner, J. (Eds.), Integrating And Applying Science: A Handbook For Effective Coastal Ecosystem Assessment. IAN Press, Cambridge, Maryland.
- Phinn, S.R., Roelfsema, C.M., Mumby, P.J., 2012. Multi-scale, object-based image analysis for mapping geomorphic and ecological zones on coral reefs. *Int. J. Remote Sens.* 33, 3768–3797.
- Radoux, J., Chomé, G., Jacques, D.C., Waldner, F., Bellemans, N., Matton, N., Lamarche, C., D'Andrimont, R., Defourney, P., 2016. Sentinel-2's potential for sub-pixel landscape feature detection. *Remote Sens.* 8, 488. <https://doi.org/10.3390/rs8060488>.
- Roelfsema, C., Phinn, S., 2010. Integrating field data with high spatial resolution multi-spectral satellite imagery for calibration and validation of coral reef benthic community maps. *J. Appl. Remote. Sens.* 4, 043527. <https://doi.org/10.1117/1.3430107>.
- Roelfsema, C.M., Phinn, S.R., Jupiter, S., Comley, J., Albert, S., 2013. Mapping coral reefs at reef to reef-system scales, 10s–1000s km², using object-based image analysis. *Int. J. Remote Sens.* 34, 6367–6388.
- Roelfsema, C.M., Kovacs, E.M., Phinn, S.R., 2017. Georeferenced Photographs of Benthic Photoquadrats Acquired Along 160 Transects Distributed Over 23 Reefs in the Cairns to Cooktown Region of the Great Barrier Reef. January and April/May, 2017. PANGAEA. <https://doi.org/10.1594/PANGAEA.877578>.
- Roelfsema, C., Kovacs, E., Ortiz, J.C., Phinn, S., Mumby, P., Callaghan, D., Ronan, M., Wolf, N., Hamylton, S., Wettle, M., 2018. Coral reef habitat mapping: a combination of object-based image analysis and ecological modelling. *Remote Sens. Environ.* 208, 27–41. <https://doi.org/10.1016/j.rse.2018.02.005>.
- Rowlands, G.P., Purkis, S.J., Riegl, B.M., 2008. The 2005 coral-bleaching event, Roatan (Honduras): use of pseudo-invariant features (PIFs) in satellite assessments. *J. Spat. Sci.* 53, 99–112.
- Roy, D.P., Li, J., Zhang, H.K., Yan, L., Huang, H., Li, Z., 2017. Examination of sentinel-2A multi-spectral instrument (MSI) reflectance anisotropy and the suitability of a general method to normalize MSI reflectance to nadir BRDF adjusted reflectance. *Remote Sens. Environ.* 199, 25–38.
- Saul, S., Purkis, S., 2015. Semi-automated object-based classification of coral reef habitat using discrete choice models. *Remote Sens.* 7, 15810.
- Smith, V.E., Rogers, R.H., Reed, L.E., 1975. Automated mapping and inventory of Great Barrier Reef zonation with Landsat data. In: Ocean 75 Conference Record. Institute of Electrical and Electronics Engineers, Inc, New York.
- Spalding, M.D., Ravilious, C., Green, E.P., 2001. World Atlas of Coral Reefs. UNEP-WCMC/University of California Press, London.
- SUHET, 2015. Sentinel-2 User Handbook, Issue 1 Revision 2. European Space Agency. <https://earth.esa.int/web/sentinel/user-guides/sentinel-2-msi>.
- UNEP-WCMC, WorldFish Centre, WRI, TNC, 2010. Global Distribution of Warm-water Coral reefs, Compiled From Multiple Sources Including the Millennium Coral Reef Mapping Project. Version 1.3. <http://data.unep-wcmc.org/datasets/1>.
- Wahidin, N., Siregar, V.P., Nababan, B., Jaya, I., Wouthuyzen, S., 2015. Object-based image analysis for coral reef benthic habitat mapping with several classification algorithms. *Procedia Environ. Sci.* 24 (Supplement C), 222–227.
- Wolff, N.H., Donner, S.D., Cao, L., Iglesias-Prieto, R., Sale, P.F., Mumby, P.J., 2015. Global inequities between polluters and the polluted: climate change impacts on coral reefs. *Glob. Chang. Biol.* 21, 3982–3994.
- Yamano, H., 2013. Multispectral applications. In: Goodman, J.A., Purkis, S.J., Phinn, S.R. (Eds.), Coral Reef Remote Sensing. vol. 3. Springer, Dordrecht, pp. 51–78.
- Yamano, H., Tamura, M., 2004. Detection limits of coral reef bleaching by satellite remote sensing: simulation and data analysis. *Remote Sens. Environ.* 90, 86–103.